Defective glycosylation of coagulation factor XII underlies hereditary angioedema type III

Jenny Björkqvist,[1,2,3] Steven de Maat,[4] Urs Lewandrowski,[5] Antonio Di Gennaro,[2,3] Chris Oschatz,[2,3] Kai Schönig,[6] Markus M. Nöthen,[7,8] Christian Drouet,[9] Hal Braley,[10] Marc W. Nolte,[11] Albert Sickmann,[5] Con Panousis,[10] Coen Maas,[4] and Thomas Renné[1,2,3]

[1]Institute of Clinical Chemistry and Laboratory Medicine, University Medical Center Hamburg-Eppendorf, Hamburg, Germany. [2]Clinical Chemistry Unit, Department of Molecular Medicine and Surgery, Karolinska Institutet, Stockholm, Sweden. [3]Center of Molecular Medicine, Karolinska University Hospital, Stockholm, Sweden. [4]Department of Clinical Chemistry and Haematology, University Medical Center Utrecht, Utrecht, Netherlands. [5]Leibniz-Institut für Analytische Wissenschaften – ISAS – e.V., Dortmund, Germany. [6]Department of Molecular Biology, Central Institute of Mental Health, Medical Faculty Mannheim, Heidelberg University, Mannheim, Germany. [7]Institute of Human Genetics and [8]Department of Genomics, Life and Brain Research Center, University of Bonn, Bonn, Germany. [9]University Joseph Fourier Grenoble, GREPI EA UJF-EFS-CNRS, National Reference Centre for Angioedema, Grenoble, France. [10]CSL Ltd., Bio21 Institute, Melbourne, Victoria, Australia. [11]CSL Behring GmbH, Marburg, Germany.

Hereditary angioedema type III (HAEIII) is a rare inherited swelling disorder that is associated with point mutations in the gene encoding the plasma protease factor XII (FXII). Here, we demonstrate that HAEIII-associated mutant FXII, derived either from HAEIII patients or recombinantly produced, is defective in mucin-type Thr309-linked glycosylation. Loss of glycosylation led to increased contact-mediated autoactivation of zymogen FXII, resulting in excessive activation of the bradykinin-forming kallikrein-kinin pathway. In contrast, both FXII-driven coagulation and the ability of C1-esterase inhibitor to bind and inhibit activated FXII were not affected by the mutation. Intravital laser-scanning microscopy revealed that, compared with control animals, both *F12*$^{-/-}$ mice reconstituted with recombinant mutant forms of FXII and humanized HAEIII mouse models with inducible liver-specific expression of Thr309Lys-mutated FXII exhibited increased contact-driven microvascular leakage. An FXII-neutralizing antibody abolished bradykinin generation in HAEIII patient plasma and blunted edema in HAEIII mice. Together, the results of this study characterize the mechanism of HAEIII and establish FXII inhibition as a potential therapeutic strategy to interfere with excessive vascular leakage in HAEIII and potentially alleviate edema due to other causes.

Introduction

Hereditary angioedema (HAE) (OMIM #106100) is a rare life-threatening inherited edema disorder that is characterized by recurrent episodes of acute swelling involving the skin or the oropharyngeal, laryngeal, or gastrointestinal mucosa (1). Increased vascular permeability in HAE is due to excessive formation of the proinflammatory peptide hormone bradykinin (BK) (2), and elevated BK plasma levels are consistently found during acute swelling attacks in HAE patients (3, 4). The serine protease activated factor XII (FXIIa) has the capacity to initiate BK formation via the kallikrein-kinin system. Contact with negatively charged surfaces induces autoactivation of zymogen factor XII (FXII) in a reaction involving high molecular weight kininogen (HK) and plasma prekallikrein (PK), collectively referred to as the plasma contact system. FXIIa cleaves PK to generate plasma kallikrein, which proteolytically liberates BK from its precursor HK (5). Binding of BK to the bradykinin B2 receptor (B2R) activates various proinflammatory signaling pathways that increase vascular permeability and fluid efflux (6). C1-esterase inhibitor (C1INH) is the major plasma inhibitor of FXIIa and kallikrein and controls activity of these contact system proteases. HAE develops in individuals who are quantitatively or qualitatively deficient in C1INH (HAE type I [HAEI] and HAEII, respectively) (1, 7); however, currently, the trigger factors for pathological BK formation and swelling attacks in HAE patients are not precisely known. Ablation of *Serping1* gene expression (which codes for C1INH) results in excessive BK production and increased vascular leakage in mice (3, 8). In contrast, mice with combined C1INH and B2R deficiency display normal vascular permeability (8). Hence, HAEI and HAEII are treated by infusion of C1INH (9) or B2R antagonist (icatibant) (10). Alternatively, the kallikrein inhibitor (DX-88; ecallantide) can be used to inhibit swelling in HAE patients (11).

In addition to these 2 classical HAE types, a third variant exists that mostly affects women. HAEIII patients exhibit recurrent episodes of swelling, although levels of fully functional C1INH are normal (Figure 1A and ref. 12). Using genome-wide linkage analyses, HAEIII was shown to be associated with a single missense mutation (c.1032C>A) in the *F12* gene (13). Independent studies involving other families found HAEIII to be associated with a different mutation affecting the same nucleotide in *F12*, c.1032C>G (14). Both point mutations translate into amino acid exchanges Thr309Lys or Thr309Arg (identical to position Thr328 if numbering includes the signal peptide). Consistent with the original nomenclature (12, 13), we here use the term HAEIII and not FXII-HAE for the HAE subtype with normal C1INH that is associated with *F12* mutations (15). *F12*-linked HAEIII is autosomal dominant inherited, and a mixture of WT and Thr309-mutated FXII circulates in plasma of HAEIII patients (13). The position Thr309 is located in the C-terminal proline-rich portion of the FXII heavy chain that mediates FXII surface-

Conflict of interest: Marc W. Nolte is an employee of CSL Behring GmbH, and Con Panousis and Hal Braley are employees of CSL Ltd.
Submitted: May 19, 2014; **Accepted:** June 4, 2015.
Reference information: *J Clin Invest*. 2015;125(8):3132–3146. doi:10.1172/JCI77139.

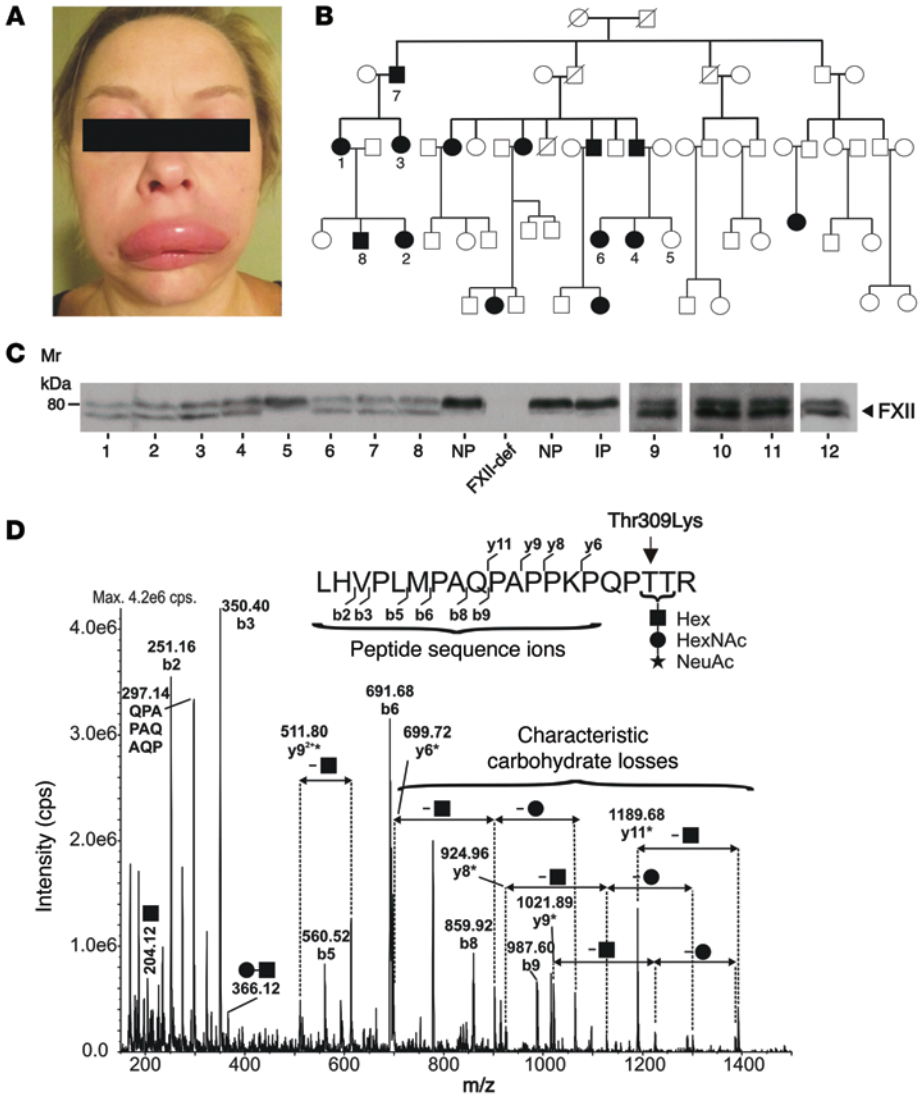

Figure 1. HAEIII patients express a FXII protein that lacks glycosylation at Thr309. (**A**) Clinical presentation of an acute swelling attack in a female HAEIII patient. (**B**) Pedigree of a French HAEIII family carrying the autosomal dominant inherited Thr309Lys FXII mutation. Squares and circles denote men and women, respectively. Black symbols represent individuals with mutation, and white symbols indicate healthy family members who do not harbor the FXII_Thr309Lys mutation. (**C**) FXII in HAEIII patient plasma samples migrates as a doublet. Plasma from HAEIII patients is indicated by 1–4 and 6–8 (**B**) and 9–12, indicating 4 HAEIII patients from unrelated families from France, Spain, and Germany. Plasma from a healthy individual (5 indicated in **B**), pooled normal plasma (NP), individual normal plasma (IP), and FXII-deficient plasma (FXII-def) are shown. A representative photographic film of $n = 3$ is shown. (**D**) Fragment mass spectrum of peptide Leu292-Arg311 being glycosylated with a HexHexNAcNeuAc glycan. A b-ion series is partially identified from b2 to b9, and several y-ions (*) corresponding to the peptide moiety, having lost the carbohydrate part, are shown. N-acetylneuraminic acid (NeuAc) is readily lost under tandem-MS conditions, and consecutive loss of hexoses and N-acetylhexosamines is observed within the y-ion series. FXII mutation Thr309Lys in the proline-rich region is indicated in the peptide sequence.

induced activation (16). Proteolysis of the peptide bond Arg353-Val354 converts FXII zymogen to the active protease FXIIa, which is composed of a heavy and a light chain. The light chain harbors the enzymatic protease domain and is linked to the heavy chain by a single disulfide bridge. Astonishingly, mutations at Thr309 (located in the heavy chain) are associated with increased FXIIa activity in HAEIII patient plasma samples (13). Here, we show that FXII mutations at position 309 in HAEIII result in the loss of an O-linked glycosylation and that this loss of glycosylation increases mutant FXII contact–induced activation. Mutant FXIIa initiates excessive BK formation in HAEIII patient plasma and edema in a genetically altered, humanized mouse model of HAEIII. Moreover, anti-FXIIa antibody attenuates pathological BK formation and inhibits aberrant vascular leakage in HAEIII.

Results

Defective FXII glycosylation in HAEIII. DNA sequencing identified the c.1032C>A mutation (which corresponds to the Thr309Lys mutation) in the *F12* genes of the HAEIII family trait. C1INH antigen and activity were in the normal range in plasma samples of carriers of the FXII mutation (Figure 1B and Supplemental Table 1; supplemental material available online with this article; doi:10.1172/JCI77139DS1). We analyzed plasma FXII in HAEIII patients and healthy family members by Western blotting with an anti-FXII antibody. FXII migrated in SDS-PAGE as a doublet in all patients (Figure 1C; 1–4, 6–8). In contrast, FXII appeared as a single band in a plasma sample of a healthy family member (Figure 1C; 5) or pooled and individual normal plasma (Figure 1C; NP, IP). Similarly, FXII migrated as a doublet using plasma collected from 4 other unrelated HAEIII patients (Figure 1C; 9–12). The upper band of the anti-FXII crossreacting material in HAEIII plasma had the same apparent molecular mass as FXII from healthy individuals, whereas the additional band was lighter. This led us to hypothesize that the Thr309 mutation interferes with posttranslational protein modifications. FXII is glycosylated at multiple sites (SwissProt entry P00748), and Thr309 is a putative O-linked glycosylation site (17). Mass spectrometry confirmed a mucin-type HexHexNAcNeuAc glycan attached to the FXII fragment peptide Leu292-Arg311 in plasma from healthy individuals (Figure 1D).

Excessive contact system activation in HAEIII plasma. We compared contact system activation in plasma of HAEIII patients and healthy controls. Samples were incubated for 30 minutes with a con-

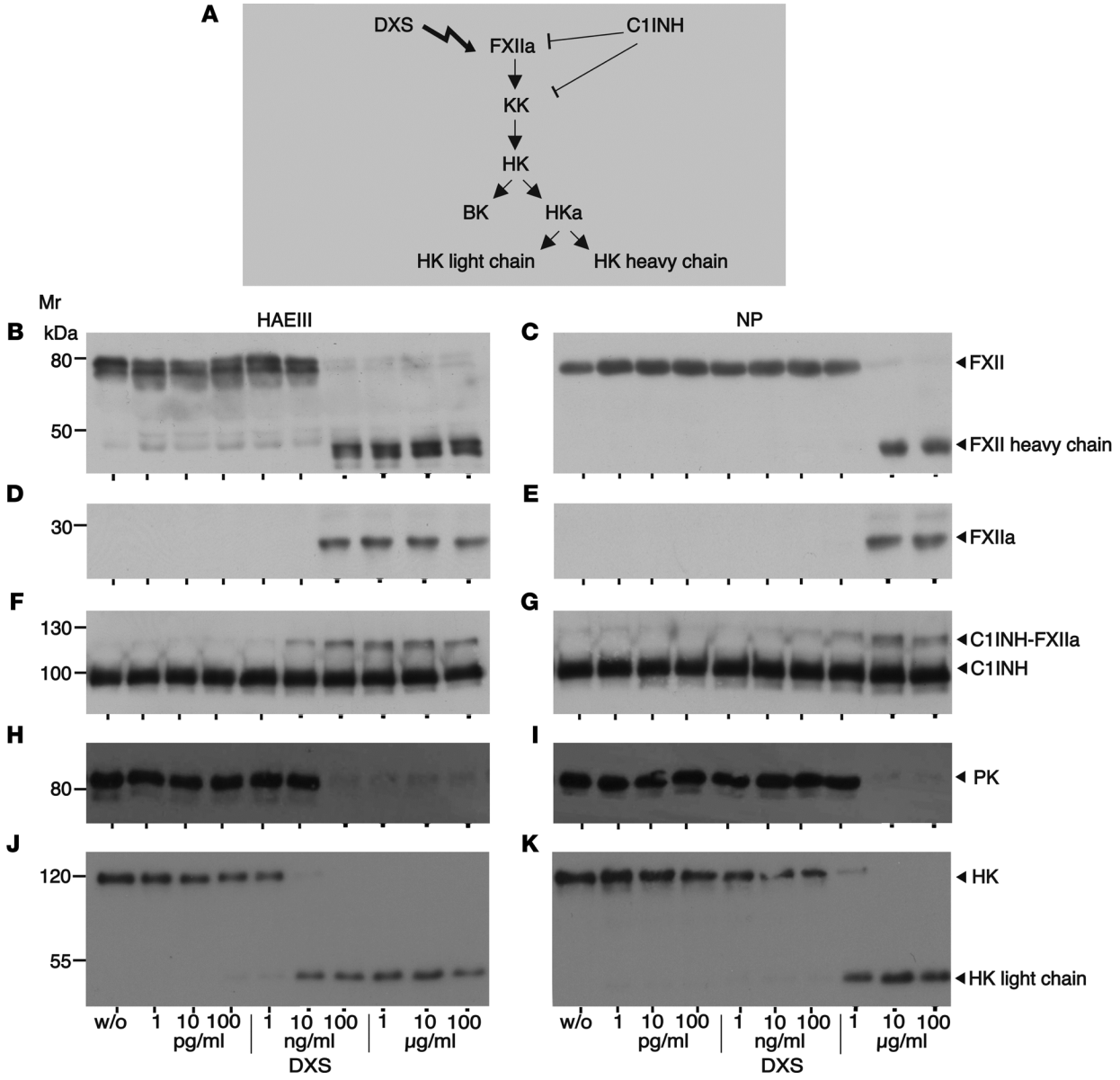

Figure 2. Increased contact system activation potential in HAEIII patients' plasma. (**A**) Schematic of the DXS-initiated contact system reaction cascade. Plasma samples from HAEIII patients and healthy controls were incubated with a concentration series of DXS (1 pg/ml-100 µg/ml) or buffer (w/o). Reduced plasma samples were analyzed by Western blotting with antibodies directed to various contact system proteins: (**B** and **C**) anti-FXII, (**D** and **E**) anti-FXIIa, (**F** and **G**) anti-C1INH, (**H** and **I**) anti-PK, and (**J** and **K**) anti-HK. A representative photographic film of a series of $n = 3$ is shown. KK, kallikrein.

centration series (ranging from 1 pg/ml to 100 µg/ml) of the FXII-contact activator high molecular weight dextran sulfate (DXS) (18) or buffer and then analyzed for zymogen FXII and PK activation, formation of FXIIa and FXIIa-C1INH complexes, and HK cleavage (Figure 2). A schematic of the DXS-triggered reaction cascade is shown in Figure 2A. In HAEIII plasma, DXS at 0.1 µg/ml or more initiated conversion of FXII to FXIIa, as indicated by disappearance of both zymogen forms (Figure 2B), concomitant with appearance of the FXIIa light chain fragment (Figure 2D). In contrast, a 100-fold higher DXS concentration was required to activate FXII in normal plasma (Figure 2, C and E). Consistent with accelerated formation of FXIIa, C1INH-FXIIa complexes formed at a much lower DXS concentration in HAEIII than in control plasma (Figure 2, F and G). Formed FXIIa initiated conversion of zymogen PK (Figure 2, H and I) and HK cleavage, as indicated by the disappearance of HK and appearance of the HK light-chain fragment (Figure 2, J and K).

Similarly, in a reconstituted plasma contact system using pure proteins (including C1INH) at plasma concentrations, DXS of 10 ng/ml or more triggered activation of FXII_Thr309Arg, formation of C1INH-FXIIa_Thr309Arg complexes, conversion of PK, and cleavage of HK. In contrast, a 100-times higher concentration of the contact activator (1 µg/ml) was required for activation of WT FXII and induction of FXIIa-driven downstream reactions (Supplemental Figure 1). Consistent with previous reports (19), mixtures of both WT and mutated FXII, PK, and HK spontaneously activated in buffer without addition of DXS. Taken together, the susceptibility for contact-initiated kallikrein-kinin system activation was enhanced in plasma from HAEIII patients over controls.

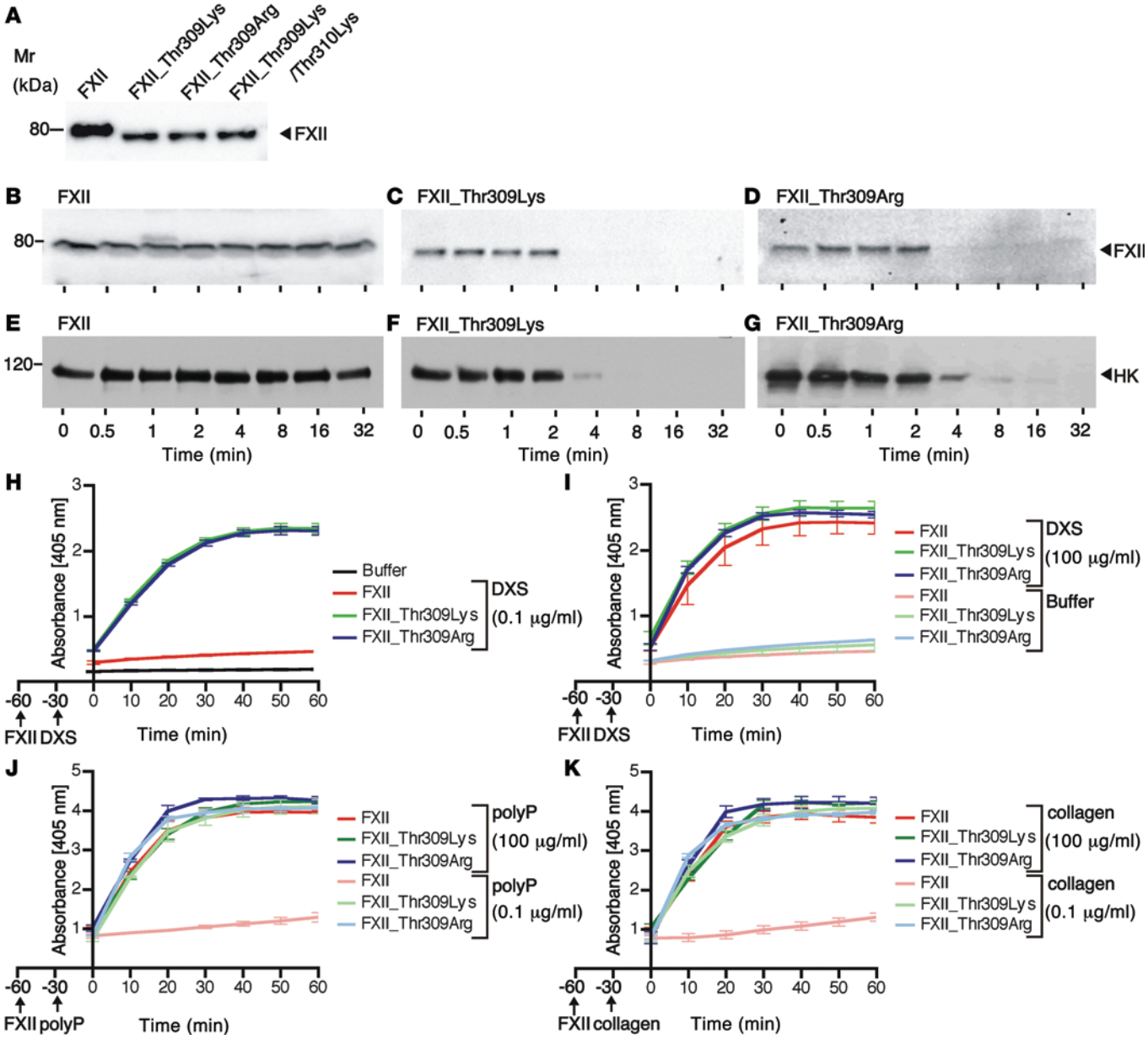

Figure 3. Thr309 mutations in FXII enhance contact activation. (**A**) Recombinant WT FXII and mutated FXII_Thr309Lys, FXII_Thr309Arg, and FXII_Thr309Lys/Thr310Lys variants were analyzed by Western blotting using an anti-FXII antibody. (**B**–**G**) FXII-deficient human plasma was reconstituted with recombinant WT FXII or Thr309-mutated FXII and activated with 0.1 μg/ml DXS. Contact-activated plasma samples were taken into reducing sample buffer at indicated time points and analyzed for cleavage of (**B**–**D**) FXII and (**E**–**G**) HK by Western blotting. $n = 3$. (**H**–**K**) FXII-deficient human plasma was reconstituted with FXII, FXII_Thr309Lys, FXII_Thr309Arg, or buffer and incubated with (**H**) 0.1 and (**I**) 100 μg/ml DXS, (**J**) 0.1 and 100 μg/ml polyP, and (**K**) 0.1 and 100 μg/ml collagen. Activity of FXIIa was measured by conversion of the chromogenic substrate D-Pro-Phe-Arg-p-nitroanilide (S-2302) at an absorption of λ=405 nm for 60 minutes. Mean ± SEM. $n = 3$.

Increased contact activation potential of recombinant FXII_Thr309 mutants. The exact site of glycosylation could not be determined from the mass spectrometry data due to the peptide fragmentation properties, but it was narrowed down to Thr309 or Thr310. To confirm that mutations at position 309 increase the potential for FXII contact activation, we cloned FXII variants and expressed Thr309Lys-, Thr309Arg-, and Thr309Lys/Thr310Lys-mutated and WT FXII in HEK293T cells. Consistent with FXII migrating as a doublet in HAEIII patient plasma, recombinant Thr309Lys-, Thr309Arg-, and the double Thr309Lys/Thr310Lys-mutated FXII variants migrated with lower apparent molecular mass than WT protein in SDS-PAGE (Figure 3A). Similar apparent molecular weight of the FXII_Thr309Lys/Thr310Lys variant as compared with FXII_Thr309Lys and FXII_Thr309Arg mutants showed that the residue Thr310 is not glycosylated in HAEIII.

To analyze the activation potential of these mutants and their capacity to induce HK cleavage, we reconstituted FXII-deficient human plasma (no detectable FXII in Western blotting) with mutated or WT FXII. When plasma, either reconstituted with FXII_Thr309Lys or FXII_Thr309Arg, was incubated with a low

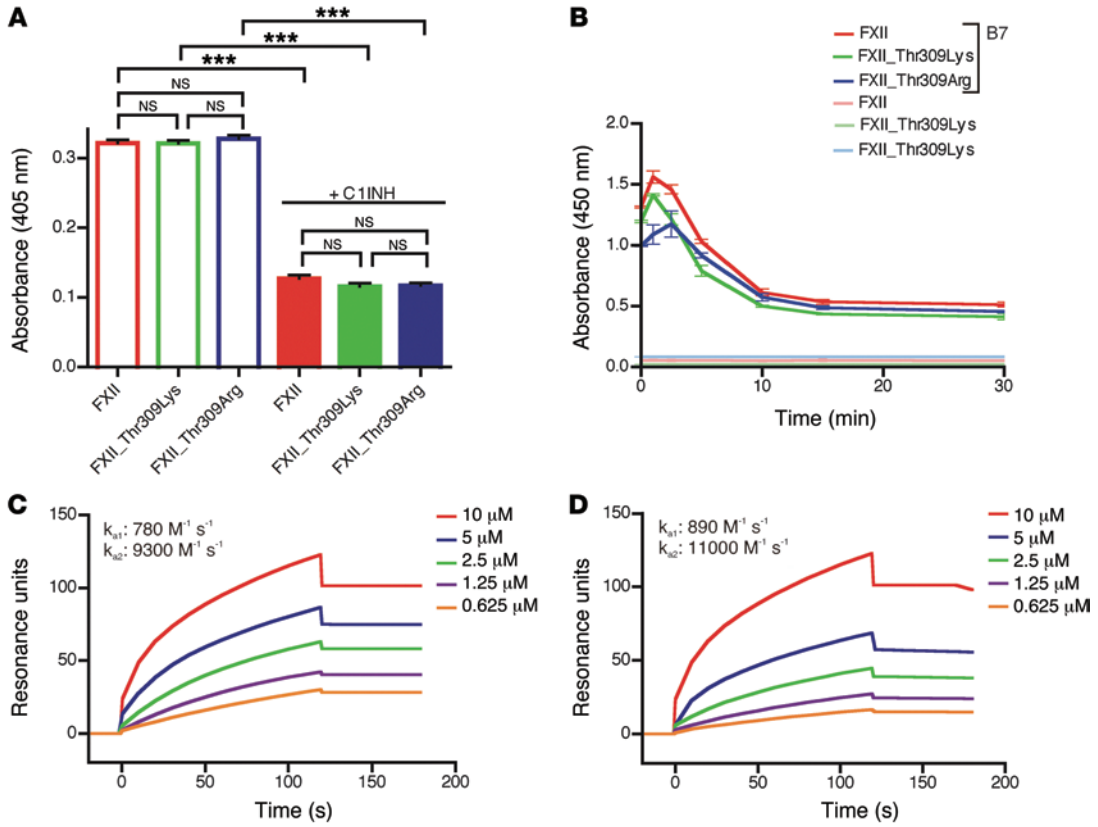

Figure 4. C1INH binds similarly to WT and mutated FXIIa. (**A** and **B**) Chromogenic substrate conversion by preactivated FXII variants. Equimolar amounts of recombinant WT FXII, FXII_Thr309Lys, and FXII_Thr309Arg were preactivated with kallikrein that was subsequently blocked by aprotinin. S-2302 chromogenic substrate was added in the absence (empty columns) or presence (filled columns) of C1INH (250 μg/ml). Bars represent the optical density at 60 minutes. Mean ± SEM. $n = 3$. ***$P < 0.001$, unpaired 2-tailed Student's t test. (**B**) Human FXII–deficient plasma was reconstituted to normal FXII plasma levels (375 nM) with purified activated WT FXIIa, FXIIa_Thr309Lys, or FXIIa_Thr309Arg and analyzed for time-dependent disappearance of FXIIa variants, indicating FXIIa-C1INH complex formation. Capture ELISA using B7 nanobody determined levels of free FXIIa in solution. Captured FXIIa was detected with a polyclonal antibody against FXII that in turn was photometrically quantified with a detection antibody and substrate reaction. Background signal in wells coated with control nanobodies (light colors). (**C** and **D**) 6xHis-tagged WT FXII and FXII_Thr309Lys proteins were immobilized on Biacore NTA sensor chips. C1INH was added in a dilution series (0.625–10 μM). Sensorgram of C1INH binding to (**C**) FXII and (**D**) FXII_Thr309Lys. Data from a single experiment that was performed 3 times are shown. Second-order rate constants were calculated from the binding data.

amount of DXS (0.1 μg/ml), both mutant FXII variants and HK were cleaved within 4 minutes. In contrast, DXS failed to initiate FXII activation and HK cleavage within 32 minutes in plasma that was reconstituted with WT FXII under the same conditions (Figure 3, B–G). These findings indicate that Thr309 mutants of FXII have increased ability to become activated at lower concentrations of negatively charged surfaces in a process called contact activation.

In chromogenic substrate conversion assays, low concentrations of DXS (0.1 μg/ml) triggered similar amidolytic activity in FXII_Thr309Lys and FXII_Thr309Arg, while the contact activator was unable to activate WT protein under these conditions (Figure 3H). In contrast, the activation of mutant and WT FXII was indistinguishable at high DXS concentrations (100 μg/ml) (Figure 3I). Similarly to DXS, low concentrations of the contact activators polyphosphate (polyP) and collagen activated FXII_Thr309Lys and FXII_Thr309Arg, but not WT FXII. For control, 1,000-fold higher levels of the contact activators initiated activation of all 3 FXII variants (Figure 3J; polyP, Figure 3K; collagen). Taken together, our data show that excess BK formation in HAEIII is due to facilitated Thr309 mutant FXII zymogen activation.

Similar C1INH binding to WT and Thr309-mutated FXIIa. To test C1INH for inhibition of WT and mutant FXIIa, we activated the zymogens by kallikrein, then inactivated kallikrein by aprotinin and analyzed enzymatic activities of formed WT FXIIa, FXIIa_Thr309Lys, and FXIIa_Thr309Arg in the absence and presence of C1INH (250 μg/ml) (Figure 4A). Substrate conversion of WT and mutant FXIIa variants was similar in the absence of C1INH. Addition of the inhibitor reduced WT FXIIa, FXIIa_Thr309Lys, and FXIIa_Thr309Arg enzymatic activities to a similar extent (31%, 29%, and 28% vs. without C1INH set to 100%). ELISA binding experiments confirmed C1INH-mediated inhibition of WT and Thr309-mutated FXIIa in a similar dose-dependent manner, with IC_{50} values (half-maximal inhibitory concentration similar to K_a values) of 95 nM each (not shown).

B7 nanobodies specifically bind to free FXIIa, but not to FXII zymogen or FXIIa-C1INH complexes (20). We compared C1INH binding to FXIIa variants using a B7-based capture ELISA. Human FXII–deficient plasma with normal C1INH levels was reconstituted with kallikrein-activated WT FXIIa, FXIIa_Thr309Lys, and FXIIa_Thr309Arg (375 nM each) and analyzed for formation of

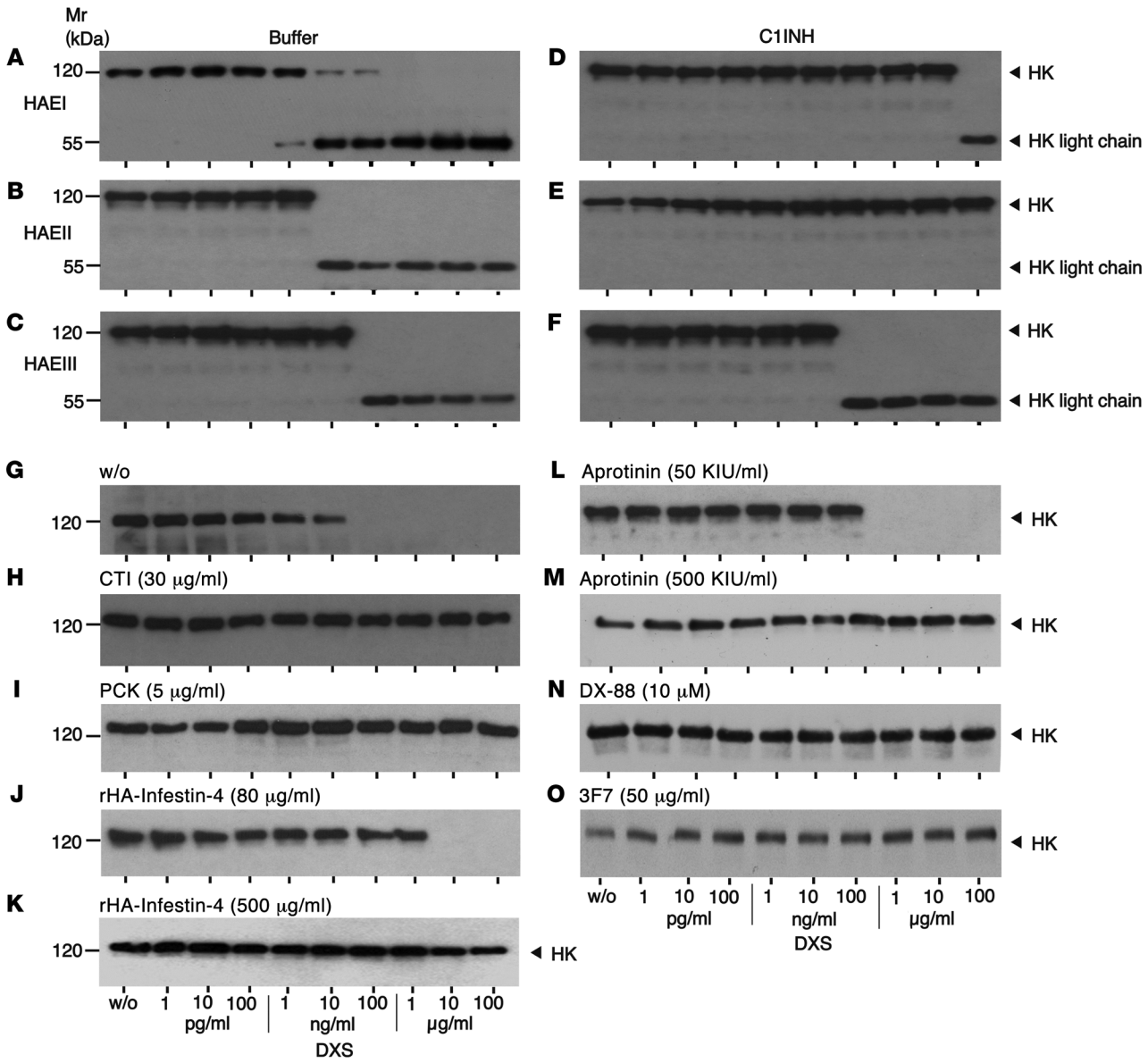

Figure 5. Inhibition of HK cleavage in plasma of HAEI, HAEII, and HAEIII patients. (**A**–**C**) Plasma samples of HAEI, HAEII, and HAEIII patients were pre-incubated with buffer or (**D**–**F**) 100 U/ml C1INH, then stimulated for 30 minutes with buffer or a concentration series of DXS (1 pg/ml-100 μg/ml) and then probed for HK (BK-containing) and the HK light chain that is generated during BK formation by Western blotting. (**G**–**O**) Inhibition of HK cleavage in HAEIII. HAEIII patient plasma was incubated with buffer or DXS (1 pg/ml-100 μg/ml) in the presence of contact system inhibitors: (**H**) CTI (30 μg/ml), (**I**) PCK (5 μg/ml), (**J** and **K**) rHA–infestin-4 (80 and 500 μg/ml), (**L** and **M**) aprotinin (50 and 500 KIU/ml), (**N**) DX-88 (10 μM), and (**O**) 3F7 (50 μg/ml). Treated plasma was analyzed by Western blotting for HK. A representative photographic film of $n = 3$ is shown.

FXIIa-C1INH complexes. C1INH bound to and inactivated WT and Thr309-mutated FXIIa in a similar fashion, indicating that HAEIII is not due to a functional C1INH deficiency (Figure 4B). To quantify C1INH inhibition of FXIIa in HAEIII, we determined the second order rate constants of C1INH binding to FXIIa variants. Surface-plasmon resonance (Biacore) was used to analyze dose-dependent interaction of C1INH with immobilized WT FXIIa (Figure 4C) and FXIIa_Thr309Lys (Figure 4D). Data fitting to a heterogeneous ligand binding model resulted in similar second-order rate constants of 780 M^{-1} s^{-1} (k_{a1}) and 9,300 M^{-1} s^{-1} (k_{a2}) for WT FXIIa and 890 M^{-1} s^{-1} (k_{a1})and 11,000 M^{-1} s^{-1} (k_{a2}) for FXIIa_Thr309Lys. C1INH binding to Thr309-mutated and WT FXIIa was comparable and consistent with previous data on WT FXIIa inhibition by C1INH (k_{a1}= 666 – 1,300 M^{-1} s^{-1} and k_{a2}= 3,800 – 7,100 M^{-1} s^{-1}; ref. 21).

FXIIa and plasma kallikrein inhibitors interfere with mutated FXII-driven HK cleavage in HAEIII. Plasma samples taken from HAEI, HAEII, or HAEIII patients were incubated with increasing concentrations of DXS and probed for HK cleavage dependent on C1INH addition. DXS of 10 ng/ml or more induced complete HK cleavage in HAEI and HAEII plasma, and a 10-fold higher contact activator concentration initiated HK conversion in HAEIII (Figure 5, A–C). C1INH addition dose dependently interfered with DXS-stimulated HK cleavage in C1INH-dependent HAEI and HAEII,

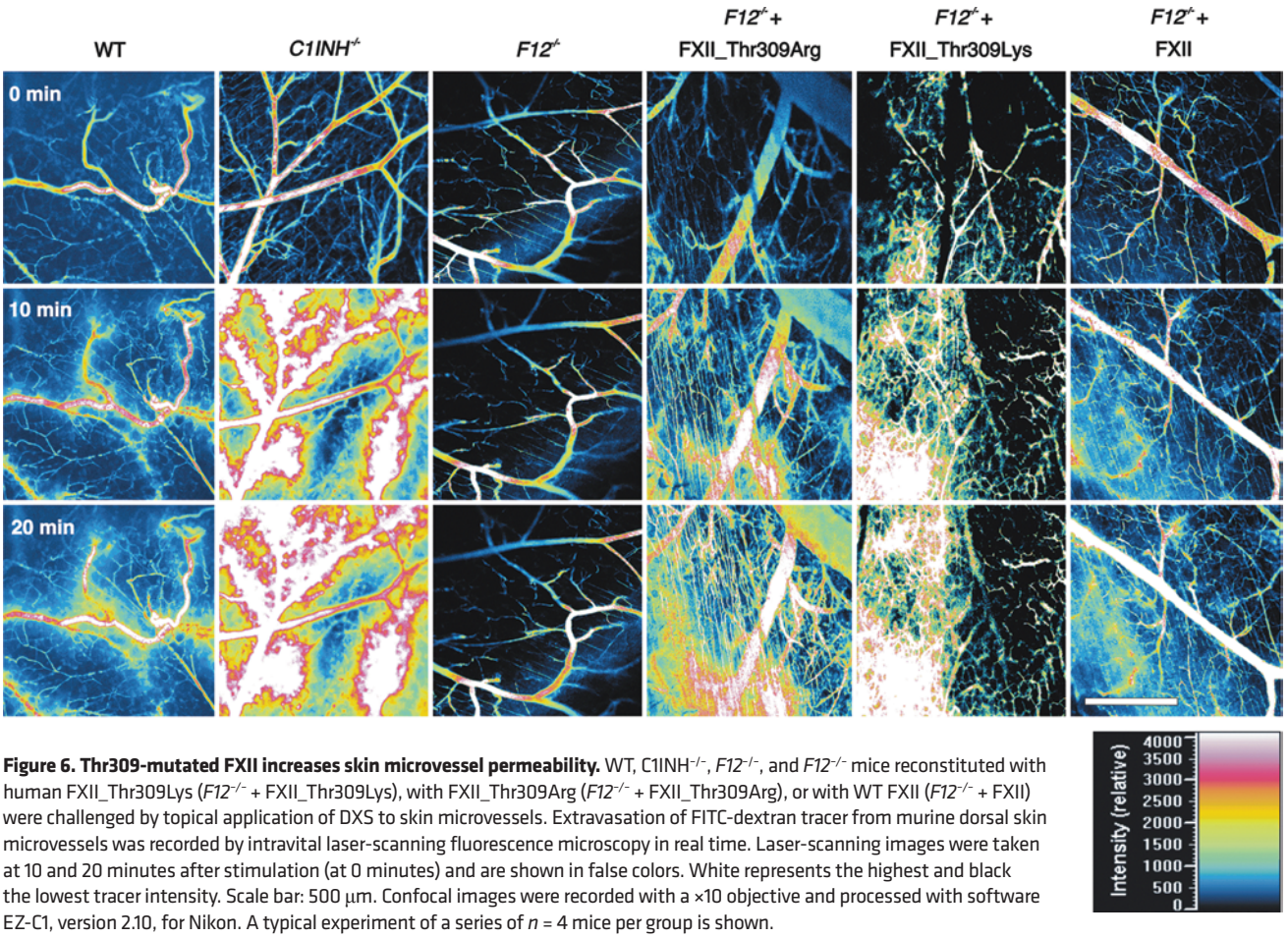

Figure 6. Thr309-mutated FXII increases skin microvessel permeability. WT, C1INH$^{-/-}$, *F12*$^{-/-}$, and *F12*$^{-/-}$ mice reconstituted with human FXII_Thr309Lys (*F12*$^{-/-}$ + FXII_Thr309Lys), with FXII_Thr309Arg (*F12*$^{-/-}$ + FXII_Thr309Arg), or with WT FXII (*F12*$^{-/-}$ + FXII) were challenged by topical application of DXS to skin microvessels. Extravasation of FITC-dextran tracer from murine dorsal skin microvessels was recorded by intravital laser-scanning fluorescence microscopy in real time. Laser-scanning images were taken at 10 and 20 minutes after stimulation (at 0 minutes) and are shown in false colors. White represents the highest and black the lowest tracer intensity. Scale bar: 500 μm. Confocal images were recorded with a ×10 objective and processed with software EZ-C1, version 2.10, for Nikon. A typical experiment of a series of n = 4 mice per group is shown.

but was largely inactive in HAEIII plasma (Figure 5, D–F). This finding motivated us to investigate alternative pharmacological strategies for interference with HK cleavage in HAEIII. The FXIIa inhibitors corn trypsin inhibitor (CTI) (30 μg/ml), H-D-Pro-Phe-Arg-chloromethylketone (PCK) (5 μg/ml), and recombinant human albumin–fused infestin-4 (rHA–infestin-4, 80 and 500 μg/ml) inhibited DXS-stimulated HK cleavage in HAEIII plasma (Figure 5, G–K). Aprotinin is used in clinical settings to interfere with kallikrein activity (22). 50 kallikrein inactivator units/ml (KIU/ml) of the inhibitor partially inhibited contact-driven HK cleavage, while 500 KIU/ml completely abrogated HK procession in HAEIII plasma (Figure 5, L and M). Similarly, the kallikrein inhibitor ecallantide (DX-88, 10 μM) blocked HK cleavage in HAEIII plasma (Figure 5N). The fully human monoclonal anti-FXIIa antibody 3F7 interferes with FXIIa-driven thrombosis in extracorporeal bypass systems (23). 3F7 inhibited contact-driven HK cleavage, and a dose of 50 μg/ml (330 nM) was sufficient to completely block plasma HK conversion (Figure 5O).

Thr309-mutated FXII increases contact-driven vascular leakage in mice. To analyze function of Thr309-mutated FXII for permeability in vivo, we infused FXII-deficient mice (*F12*$^{-/-}$) with recombinant FXII_Thr309Lys, FXII_Thr309Arg, or WT FXII. All these reconstitutions normalized the prolonged activated partial thromboplastin time (aPTT, a measure for the FXIIa-driven intrinsic coagulation pathway) of *F12*$^{-/-}$ mouse plasma close to WT animal levels (85 ± 22 to 28 ± 11 for Thr309Lys, 30 ± 7 for Thr309Arg vs. 26 ± 6 seconds for WT). We analyzed vascular leakage in reconstituted animals by real-time intravital confocal laser-scanning microscopy. FITC-dextran was intravenously injected as a macromolecular tracer for plasma protein extravasation. A ventral skin window was incised, and skin was inverted and analyzed under the microscope. No basal extravasation of the tracer was detectable 5 minutes prior to stimulation, indicating intact vascular barriers. Topical application of DXS provoked leakage in WT mice. The first leaky spots appeared within 10 minutes, and leakage was maximal after 20 minutes (tracer fluorescence intensity 10.5 ± 1.4-fold of initial t = 0 minutes signal; Figure 6, WT). Consistent with heparin-driven increase in vascular permeability (24), DXS-stimulated leakage in C1INH$^{-/-}$ mice (a mouse model for HAEI) was excessive (34.3 ± 3.9-fold; Figure 6) and occurred more rapidly than in WT animals. In contrast, *F12*$^{-/-}$ mice were resistant to DXS-stimulated increase in vascular permeability (1.1 ± 0.4-fold; Figure 6). Contact-induced leakage was largely increased in both FXII_Thr309Arg- and FXII_Thr309Lys-reconstituted *F12*$^{-/-}$ mice and exceeded WT mouse levels by approximately 3-fold (25.7 ± 3.9-fold and 24.2 ± 2.4-fold; Figure 6). Kinetics and magnitude of DXS-triggered tracer extravasation did not differ between the 2 mutant FXII-reconstituted mouse lines. Increase of permeability in normal human FXII–reconstituted animals was similar to

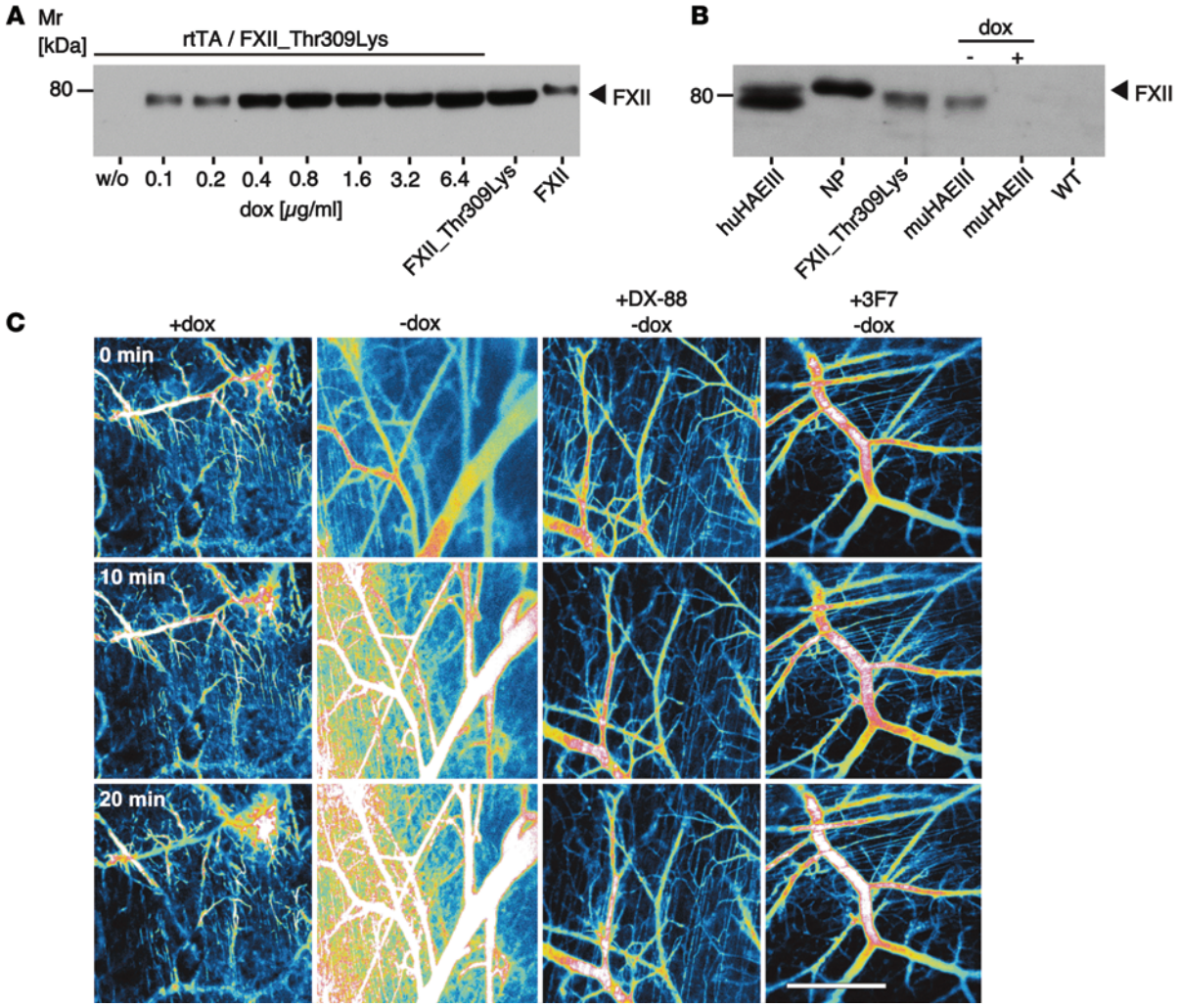

Figure 7. Increased vascular leakage in HAEIII mice. (**A**) Inducible expression of FXII_Thr309Lys in HEK293T cells, incubated in the presence of increasing concentrations of doxycycline (dox; 0.1–6.4 μg/ml) or buffer using a Tet-On system. FXII_Thr309Lys in supernatants was analyzed by Western blotting after 48 hours of induction. FXII and FXII_Thr309Lys were loaded as controls. $n = 3$. (**B**) Transgenic FXII_Thr309Lys expression was induced in HAEIII mice (Tet-Off system) by dox withdrawal (–) and suppressed by dox (+). Plasma samples from induced (–dox) and noninduced (+dox) HAEIII mice (muHAEIII) were analyzed by Western blotting using a human anti-FXII antibody that does not crossreact with the mouse orthologue. Plasma samples from a HAEIII patient (huHAEIII), a healthy individual (NP), a WT mouse, and HEK293T cell–expressed FXII_Thr309Lys were loaded for comparison. (**C**) Extravasation of FITC-dextran tracer from murine dorsal skin microvessels was recorded by intravital laser-scanning fluorescence microscopy in real time. DXS was topically applied to the inverted skin of either noninduced (+dox; not expressing FXII_ Thr309Lys) or induced (–dox; expressing FXII_ Thr309Lys) HAEIII mice (columns 1 and 2). HAEIII mice expressing FXII_Thr309Lys were injected with DX-88 (430 μg/kg bw) or 3F7 (7 mg/kg bw) 30 minutes before FITC-dextran application (columns 3 and 4). Laser-scanning images were taken at 10 and 20 minutes after stimulation by topical application of DXS to skin microvessels at time point 0 minutes and are shown in false colors. White represents the highest and black the lowest tracer intensity. Scale bar: 500 μm. $n = 4$ per group.

WT mouse levels (10.1 ± 2.3-fold, $P > 0.05$ vs. WT; Figure 6). There was no obvious sex difference in contact system–mediated leakage for all mouse strains investigated.

Increased vascular leakage in a HAEIII mouse model. We next generated a mouse model of HAEIII with liver-specific inducible expression of human FXII_Thr309Lys on a *F12* heterozygous genetic background ($F12^{+/-}$). First, we analyzed inducible expression of FXII_Thr309Lys in transfected HEK293T cells using the Tet-On system. Western blotting showed doxycycline dose–dependent expression of the construct. The recombinant mutant FXII migrated at a lower apparent molecular weight than WT FXII and apparent molecular weight was identical to HAEIII patient plasma–derived FXII_Thr309Lys, indicating impaired glycosylation (Figure 7A).

For doxycycline-controlled in vivo expression of FXII_Thr309Lys, we used the Tet-Off system that requires 2 transgenic mouse strains enabling liver-specific transgene expression in the absence of the inducer. We generated a transgenic mouse line that expresses FXII_Thr309Lys under the control of a tetracycline-responsive element (TRE). These transgenic animals were crossed with a second mouse strain that expresses the tetracycline-controlled transcriptional activator (tTA) under the control of the liver-specific LAP promoter (25). Resulting double-transgenic animals were bred with $F12^{-/-}$ mice to reduce expression of endogenous FXII to 50% of WT mouse levels (26). The breeding led to HAEIII mice that expressed 50% of normal plasma levels of endogenous (murine) FXII and, in addition, human FXII_Thr309Lys only in

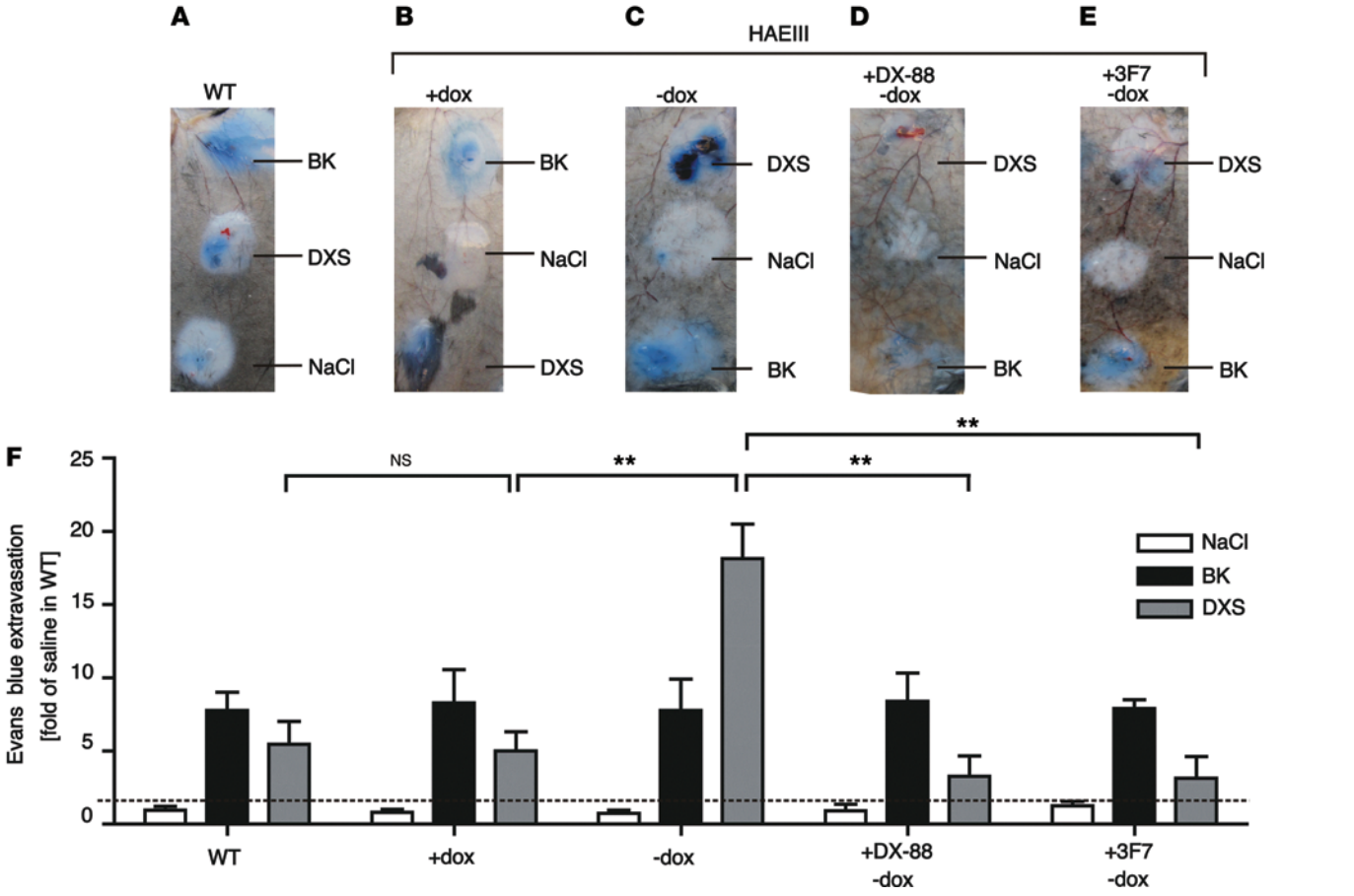

Figure 8. Increased DXS-driven edema in HAEIII mice. (**A**–**E**) Evans blue was intravenously infused as a tracer into (**A**) WT, (**B**) noninduced HAEIII (+dox), and (**C**) induced HAEIII (–dox) mice, and (**D** and **E**) FXII_Thr309Lys–expressing mice treated with DX-88 (430 μg/kg bw; +DX-88 –dox) or 3F7 (7 mg/kg bw; +3F7 –dox). Skin edema formation was induced by intradermal injection of 50 μl BK (100 μM), DXS (80 mg/ml), or saline as control (NaCl) and visualized by tracer extravasation after 30 minutes. (**F**) Spots with extravasated tracer were excised entirely, and dye was extracted and quantified. Tracer extravasation is plotted relative to leakage in WT mice stimulated with NaCl (dashed line). Columns show mean ± SEM. $n = 4$ per group.**$P < 0.01$, unpaired 2-tailed Student's t test. Representative mouse hides are shown in **A**–**E**.

the absence of doxycycline (when tTA activated expression of the transgene) specifically in hepatocytes (where the LAP promoter was active) (Supplemental Figure 2, A and B). Plasma samples from HAEIII mice were analyzed for FXII_Thr309Lys using an anti-FXII antibody that specifically binds to human FXII (WT and mutated protein) and does not recognize the murine homolog (Figure 7B). Transgenic mutant FXII expression was suppressed by supplementing mouse food with doxycycline. FXII_Thr309Lys in HAEIII mouse plasma migrated at the same apparent molecular weight as patient-derived and HEK293T-expressed proteins (Figure 7B; lanes 1, 3, and 4) and at a lower weight than that seen in normal FXII from healthy individuals (Figure 7B; lane 2).

We compared vascular leakage in HAEIII mice dependent on FXII_Thr309Lys expression. There was no detectable basal leakage without stimulation in HAEIII mice within 30 minutes. DXS-induced leakage was increased more than 3-fold (27.3 ± 3.5-fold vs. 7.4 ± 1.5-fold, $t = 20$ minutes, Figure 7C, +dox vs. –dox) in HAEIII mice that express FXII_Thr309Lys over their nonexpressing counterparts. Vessel permeability in HAEIII mice was similar to the leakage in C1INH$^{-/-}$ mice (27.3 ± 3.5-fold, NS vs. C1INH$^{-/-}$; Figure 7C, –dox vs. Figure 6, C1INH$^{-/-}$), whereas vascular leakage in the absence of FXII_Thr309Lys expression did not differ from WT mouse levels (7.4 ± 1.5-fold; NS vs. WT; Figure 7C, +dox vs. Figure 6, WT). Targeting kallikrein and FXIIa interfered with excessive contact system activation in HAEIII patient plasma (Figure 5, N and O). We next investigated whether inhibition of kallikrein or FXIIa had therapeutic potential in our HAEIII mouse model. DX-88 (430 μg/kg body weight [bw]) or anti-FXIIa antibody 3F7 (7 mg/kg bw) was intravenously infused into HAEIII mice (that expressed FXII_Thr309Lys) 5 minutes prior to DXS application. Both inhibitors fully blocked DXS-induced vascular leakage, and permeability was as low as in *F12*$^{-/-}$ mice in both cases (2.8 ± 1.4-fold [DX-88] and 1.4 ± 1.1-fold [3F7]; NS vs. *F12*$^{-/-}$ [1.1 ± 0.4-fold], Figure 7C, +DX-88 –dox and +3F7 –dox).

Increased edema formation in a HAEIII mouse model. We analyzed the contribution of FXII_Thr309Lys to vascular leakage in mice using an alternative technique, the Miles edema model (27). This model allowed us to spectrophotometrically quantify the amount of extravasated Evans blue dye in excised skin samples after intradermal injections with stimuli. Basal vascular permeability, assessed in saline-injected skin, was low (≤1.5) in all mice tested. BK stimulated similar leakage in WT and HAEIII

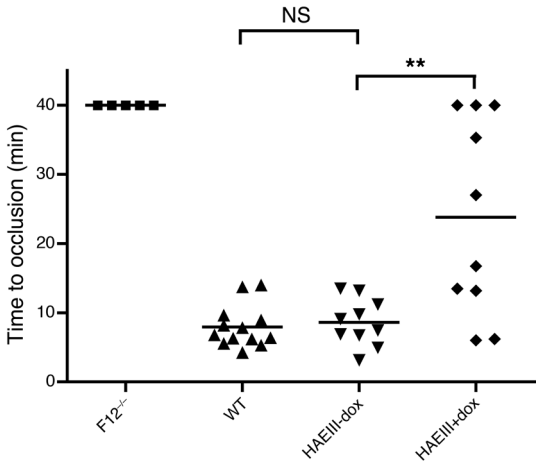

Figure 9. Thrombus formation in HAEIII mice. Thrombosis was induced in the carotid artery of *F12*$^{-/-}$, WT, HAEIII –dox (induced) and HAEIII +dox (noninduced) mice by topical application of 5% $FeCl_3$ for 3 minutes. Time to complete vascular occlusion after injury was monitored. Each symbol represents 1 individual animal. The experiment was stopped after 40 minutes. $^{**}P < 0.01$, unpaired 2-tailed Student's *t* test.

mice (Figure 8, A–E). Dye extravasation was plotted relative to the saline-induced signal in WT mice (WT set to 1.0, Figure 8F). Increase in vessel permeability after BK injection in HAEIII mice was similar to leakage in WT mice and was independent of FXII_Thr309Lys expression (7.8 ± 2.1 [+dox] and 8.3 ± 2.2 [–dox], vs. 7.8 ± 1.2 [WT]; $P > 0.05$ HAEIII vs. WT; reported as the fold change in Evans blue extravasation compared with WT mice injected with saline here and below). As expected, inhibition of kallikrein or FXIIa (by infusion of DX-88 or 3F7, respectively) did not reduce BK-induced leakage in the skin of FXII_Thr309Lys-expressing HAEIII mice (8.3 ± 1.9 [DX-88]; 7.9 ± 0.6 [3F7]; $P >$ 0.05 vs. WT). Consistent with previous studies (17), intradermal injection of DXS induced leakage in WT mice (5.5 ± 1.6). DXS-triggered vascular permeability was increased more than 3-fold in FXII_Thr309Lys-expressing HAEIII animals compared with non-induced HAEIII mice (18.1 ± 2.4 vs. 5.0 ± 1.3; $P < 0.01$), and the contact activation-induced leakage was similar in noninduced HAEIII versus WT mice. Since congenital deficiency in B2R provides protection from contact system–mediated edema (24), we further tested the therapeutic potential of inhibitors of BK formation in our new mouse model of HAEIII. Infusion of DX-88 or 3F7 prior to challenge largely reduced DXS-induced edema in FXII_Thr309Lys-expressing induced HAEIII mice (3.3 ± 1.4 [DX-88] and 3.1 ± 1.5 [3F7]; $P < 0.01$ vs. untreated HAEIII mice). Leakage in inhibitor-pretreated HAEIII mice was below challenged WT mouse levels, suggesting that inhibitors interfered with mutant and endogenous FXIIa-driven increases in vascular permeability. Cumulatively, these data show that FXII_Thr309Lys mediates increased contact-initiated vascular leakage in vivo.

Normal arterial thrombus formation in HAEIII mice. Thrombin generation in HAEIII patient plasma triggered by contact activators kaolin and ellagic acid is indistinguishable from that of healthy controls (Supplemental Figure 3). Consistent with previous data (28), the aPTT in HAEIII patient plasma is within the reference range (33 ± 4, 25–38 seconds) indicating that FXII, PK, and HK plasma antigen levels are normal. Western blotting with contact factor–specific antibodies (29) confirmed comparable FXII, PK, C1INH, and HK plasma levels in HAEIII patients and healthy controls (not shown). Consistent with the results in patients, the aPTT in plasma of induced HAEIII mice was close to WT animal levels (30 ± 8 vs. 26 ± 6 seconds). Arterial thrombus formation induced by mechanical vascular injury is defective in *F12*$^{-/-}$ mice (26). Thrombosis in the carotid artery challenged with $FeCl_3$ was consistently impaired in *F12*$^{-/-}$ mice, and all animals displayed normal flow rates through the injured vessel at the end of the 40-minute observation period. Thrombus formation in induced HAEIII mice was not significantly different from that of WT animals, and arteries occluded in all mice within 15 minutes (8.5 ± 1.1 vs. 7.9 ± 0.8 minutes, $n = 10$). Noninduced HAEIII mice did not express human FXII_Thr309Lys and exhibited 50% of endogenous FXII levels only. In these animals, 7 to 10 carotid vessels occluded and time to occlusion was prolonged (23.8 ± 4.5 minutes, Figure 9).

Discussion

Classical HAEI and HAEII result from a deficiency in functional C1INH (30) and occur with roughly the same prevalence of 1 in 50,000 to 100,000 in men and women (31). In contrast, C1INH-independent HAEIII was initially believed to selectively affect women in an estrogen-dependent manner (12). Challenging the suggested X-linked dominant mode of inheritance, genome-wide linkage studies associated HAEIII with a single-point mutation in the *F12* gene on chromosome 5 (13); recently, male HAEIII patients were identified (32, 33).

Here, we show that both HAEIII-associated FXII mutations Thr309Lys (13) and Thr309Arg (14) result in a loss of O-linked glycosylation that increases their susceptibility for contact activation compared with healthy controls, notwithstanding the mutation being located outside the enzymatic domain. We reasoned that mutations at position Thr309 could increase susceptibility of contact-induced FXII zymogen activation or modulate the interaction of FXIIa with inhibitors such as C1INH. The FXII mutation did not affect C1INH binding, as second-order rate constants for C1INH inhibition of Thr309-mutated and WT FXIIa were similar and consistent with previous data for WT protein inhibition by C1INH on cell surfaces (21). FXII binds to surfaces via its heavy chain, and surface-bound FXIIa is protected from inactivation by C1INH. The heterogeneous ligand-binding model used in surface plasmon resonance (SPR) analysis reflects these 2 populations of FXIIa molecules, either surface associated via a combination of the heavy chain and 6xHis-tag or simply via the tag alone (21). Consistent with the surface-plasmon resonance data, C1INH bound and inhibited WT and mutated FXIIa forms similarly in plasma (Figure 4) and immobilized on surfaces (IC_{50} of 95 nM). The data argue against a postulated role of increased C1INH binding to mutated FXIIa variants for pathological BK formation in HAEIII (34).

CTI (a FXIIa inhibitor) prevents FXIIa-C1INH complex formation; however, it does not inhibit FXIIa-mediated PK activation, indicating that C1INH binding to WT FXIIa is slow compared with FXIIa-triggered PK-mediated HK processing (35). Facilitated formation of the mutated enzyme and slow inhibition of the active protease offers an explanation for poor interference of C1INH

with Thr309-mutated FXIIa-initiated BK formation. While contact-triggered Thr309-mutated FXIIa formation escaped the control of C1INH, the inhibitor inactivated both preformed WT and Thr309-mutated proteases (Figure 5). C1INH has been reported to inhibit edema in some HAEIII patients (36), and interference of C1INH with excessively formed kallikrein and Thr309-mutated FXIIa offers a rationale for this activity.

Activation of FXII_Thr309Lys or Thr309Arg mutants initiated by naturally occurring and synthetic contact activators was increased in both plasma and a purified system containing physiological levels of C1INH (Figure 3 and Supplemental Figure 1). Thus, HAEIII appears to be caused by a hyperactivable FXII_Thr309Lys or FXII_Thr309Arg that has enhanced susceptibility for contact activation over WT FXII. This excessive activation of mutant FXII induces edema in a BK-dependent manner via the kallikrein-kinin pathway in vivo. Consistently, targeting FXIIa or kallikrein interferes with pathological vascular leakage in HAEIII. HAEIII patient FXII plasma levels and total FXIIa enzymatic activity (following full activation) were in the normal range. However, Thr309-mutated FXII variants showed increased susceptibility for contact activation over the WT protein. This may help explain why the aPTT assay, which measures total FXII activity levels in response to excess stimulation with the strong contact activator silica, is normal in HAEIII patients (28). In support of the notion that FXII is more easily contact activated in HAEIII, doses of DXS that are insufficient to trigger FXIIa formation in healthy individuals readily activate FXII_Thr309Lys and produce BK in HAEIII patient plasma (Figure 2) and BK-dependent vascular leakage in HAEIII mice (Figure 6). Recently, the crystal structure of the FXIIa protease domain was solved (37). The structure improves understanding of FXIIa interaction with inhibitors and substrates; however, the insect cell–expressed construct does not comprise the residue Thr309.

FXIIa (38) and FXIIa-C1INH complexes (39) are significantly increased in the acute swelling episode, but not during remission, in HAE patient plasma. Consistent with findings in HAEI and HAEII patients (40), we found contact system factor consumption in 3 of our HAEIII patients during the acute swelling episode, supporting FXIIa-driven BK formation in HAE. However, in addition to FXIIa and contact activation, alternative mechanisms of BK formation might exist with potential implications for HAE. PK- and HK-deficient mice have very low levels of BK (41, 42). In contrast, inherited FXII deficiency reduces baseline BK plasma levels by 50% only, indicating FXII-independent BK formation in these mice (43). Proteases, such as neutrophil elastase and mast cell–derived tryptase, process HK and might have a role in BK formation at sites of inflammation involving activated mast cells (44). Furthermore, BK formation mediated by zymogen PK bound to HK has been described in plasma of HAEI and HAEII patients. The underlying mechanism has remained enigmatic and may involve defective stabilization of PK-HK complexes in the absence of C1INH (19, 45).

Similarly to Thr309 in human FXII, differential glycosylation has been implicated in contact system regulation in rodents. Lewis rats are more susceptible to the development of inflammation in bacterial-induced colitis (46) and B2R-mediated inflammatory arthritis models (47). In contrast to other rat strains, Lewis rats lack an O-linked glycosylation in HK and have an increased rate of HK cleavage by kallikrein during activation by DXS (48).

We focused on the 2 FXII mutations at Thr309 that were initially described in HAEIII families (13, 14). Recently, a *F12* gene deletion of 72 base pairs (coding amino acids 305–321) was identified in 2 unrelated HAEIII families (49, 50). Additionally, in a 37-year-old woman and her daughter with recurrent C1INH-independent angioedema, a duplication of 18 base pairs in the *F12* gene was reported (51). This duplication codes for 6 additional amino acids in FXII (positions 298–303). The molecular mechanism of edema formation in patients carrying these latter 2 mutations is unknown. However, all mutations in C1INH-independent HAEIII patients affect the proline-rich region of FXII. This C-terminal portion of the FXII heavy chain mediates contact to other proteins and zymogen FXII surface binding (16), supporting a critical function of Thr309 for zymogen contact activation. In contrast with gain-of-function FXII mutations associated with edema, multiple other mutations are known to cause loss of FXII activity. Some of these mutations reduce FXII plasma levels by interference with synthesis or secretion (52). Other mutations reduce the enzymatic activity of FXIIa; these are mostly located in the serine protease catalytic triad His393-Asp442-Ser544 or are close to the active site (52). Another example is FXII Locarno, which is a secreted but dysfunctional protein, due to an Arg353Pro substitution mutation. The mutation alters the FXIIa/kallikrein recognition site in FXII and abolishes zymogen activation by limited proteolysis (53).

The proline-rich region mediates the binding of FXII to negatively charged surfaces, which triggers a conformational change to induce FXII activation (autoactivation) (16). Activation of FXII by the silicate kaolin is used to initiate the FXIIa-driven intrinsic coagulation cascade in aPTT coagulation assays (5, 54). FXIIa cleaves surface-associated PK to generate kallikrein, which in turn reciprocally activates further FXII molecules, thereby amplifying the initial signal (5, 54, 55). In vitro, the polyanionic polysaccharide heparin liberates BK by providing a surface for FXII contact activation (56, 57). We have recently identified mast cell–released heparin as an endogenous FXII activator during mast cell–mediated vascular leakage in a mouse model of HAEI (24). Additionally, heparin triggers BK-mediated hypersensitivity reactions, including hypotension in mouse models of anaphylaxis and in anaphylactic patients in an FXII-dependent manner (29). Cutaneous edema in HAEIII patients is known to occur after allergen exposure or physical stress (36), which is associated with degranulating mast cells (58). Heparin specifically triggers FXIIa-mediated BK formation; however, under these conditions, FXIIa does not trigger the intrinsic coagulation pathway via its substrate FXI (24). HAE patients suffer from recurrent activation of FXII and consecutively BK-mediated swelling, but the swelling episodes are not associated with an enhanced risk for thrombosis (59). FXII contact activators either trigger activation of both coagulation and kallikrein-kinin systems or specifically activate the kallikrein-kinin pathway without activating coagulation (54). For example, misfolded protein aggregates allow for FXIIa and kallikrein without activation of coagulation, indicating that some biological surface initiates inflammatory events in an FXIIa-dependent manner independently of coagulation (24, 60). Similarly to mast cell–released heparin, the synthetic polysaccharides oversulfated chondroitin sulfate (61) and DXS (62) specifically

trigger BK formation in patients and large animal models without producing thrombotic reactions in vivo. Other contact system activators such as polyP (63) or ellagic acid initiate both FXIIa-driven fibrin and BK formation. The precise molecular basis for the preferential activation of the kallikrein-kinin pathway, without the intrinsic coagulation pathway, requires further investigation and may involve differential proteolysis forms of FXIIa (64), additional FXIIa substrates, FXIIa-independent BK-forming reactions, or the nature and structural requirements of the FXII zymogen-activating surface (60, 64).

There has been substantial progress in the development of therapeutic targets for HAE. Current treatments of choice for acute edema attacks are supplementation of C1INH (9), inhibition of kallikrein (DX-88, ecallantide) (11), and targeting of B2R (icatibant) (10). All these pharmacological strategies interfere with FXIIa-initiated BK function. In contrast to all other coagulation proteases, inherited FXII deficiency is not associated with any hemorrhagic disorder in humans, baboons, birds, or mice. While being dispensable for hemostasis (5) in mouse (26) and large animal models (65), there is a critical role of FXII in thrombosis, making it an attractive antithrombotic drug target. The recombinant FXIIa-specific antibody 3F7 blocks FXIIa activity and prevents surface-induced clotting of plasma. Infusion of 3F7 provides thromboprotection in a clinical setting without therapy-associated increase in bleeding. Additionally, targeting FXIIa with 3F7 interferes with DXS-driven contact activation in human plasma (23) and edema formation in HAEIII mice (Figure 8). This suggests that the fully human antibody 3F7 may be useful both in the prophylaxis and acute settings of HAE. Indeed, humanized antibodies have been effectively introduced as patient therapy on numerous occasions (66). Similarly, subcutaneous application of fully human anti-kallikrein antibody DX-2930, which has a high bioavailability (66%) and long half-life (12.5 days), interferes with BK formation in monkeys. A placebo-controlled, dose-escalation phase 1 trial with DX-2930 has just been completed (67). Antisense oligonucleotides (ASOs) provide an alternative method to interfere with PK and FXII activity. Repetitive subcutaneous ASO injection knocks down FXII and/or PK expression for several weeks in mice (68). Contact-induced leakage in WT and *F12*$^{+/-}$ mice (having 50% FXII plasma levels of WT animals) (26) are similar (Figure 7), indicating that half-normal FXII levels are sufficient for edema formation. Consistently, FXII levels of 50% also allow for thrombus formation (69), emphasizing the need for potent and selective FXIIa-interfering therapeutic strategies. Clinical studies are required to evaluate and compare the efficacy and applicability of these new agents in patients of various HAE types.

This study shows that the mechanism for HAEIII is increased contact-activatable FXII, resulting from a defective O-linked Thr309 glycosylation, which leads to BK formation in vitro and angioedema in vivo.

Methods

Patients. HAEIII plasma samples were obtained from France, Germany, and Spain. Control plasma was obtained from healthy volunteers at the Karolinska University Hospital or purchased from Siemens Life Science. FXII-deficient human plasma was obtained from George King Bio-Medical Inc.

Genotyping of HAEIII patients. *F12* gene sequencing was performed in symptomatic HAEIII patients and in unaffected relatives. DNA was extracted from venous EDTA anticoagulated blood using a DNA extraction kit (DNeasy Blood and Tissue Kit, QIAGEN). PCR was performed using forward primer 5′-ACGTGACTGCCGAGCAAG-3′ and reverse primer 5′-CCTCTCGGCTCCTCCTTC-3′ with 30 cycles with an annealing temperature of 59°C. The mutation was confirmed by sequencing.

Peptide analysis by mass spectrometry. Tryptic peptides from in-gel digestion of 1D-PAGE bands were separated by nano-LC and detected by a Qtrap4000 Mass Spectrometer (Applied Biosystems) as previously described (70).

Contact phase system activation assays in vitro. Human citrated platelet-poor plasma samples were activated with increasing concentrations (ranging from 1 pg/ml to 100 μg/ml) of high molecular weight DXS (500 kDa, Sigma-Aldrich) or buffer in the presence or absence of C1INH concentrate (Berinert, CSL Behring GmbH); FXIIa inhibitory antibody (3F7, CSL Limited); PCK (Bachem); rHA–infestin-4 (CSL Behring GmbH); CTI (Calbiochem); aprotinin (Trasylol, 500,000 KIU, Bayer) or DX-88 (Ecallatide, Dyax). Similarly, a reaction containing recombinant expressed pure FXII or FXII_Thr309Arg, HK (Molecular Innovation), PK (Molecular Innovation), and C1INH (Berinert) was supplemented with DXS. Samples were incubated for 30 minutes at 37°C. Reducing Laemmli sample buffer was added to stop reactions, and the samples were boiled for 5 minutes followed SDS-PAGE on 8% gels and Western blotting using the following antibodies: anti-FXII; anti-C1INH (catalog GAHu/FXII and GAHu/CEI; Nordic Immunological Laboratories); anti-FXIIa (29), donated by David Pritchard, Axis Shield, Dundee, United Kingdom); anti-HK (71, 72), or anti-PK antibody (catalog SAPK-AP; Affinity Biologicals Inc.). All antibodies were diluted 1:1000 and horseradish peroxidase–coupled secondary antibody was diluted 1:5000 (catalog 205-032-176 and 713-035-147; DAKO).

FXIIa amidolytic activity assays. FXII-deficient plasma was reconstituted with mutated or WT FXII and stimulated with DXS, polyP (>150 phosphate units, BK Guilini), or collagen (Collagen Reagens HORM, Takeda). The enzymatic activity of FXIIa was measured photometrically using the chromogenic substrate S-2302 (1 mM, Chromogenix) at an absorbance wavelength of 405 nm. In another set of experiments using pure proteins, FXII was activated with kallikrein for 15 minutes, aprotinin was added to inhibit kallikrein, and then C1INH or buffer was added together with the chromogenic substrate L2120 (H-D-Pro-Phe-Arg-pNA, 2.5 mM, Bachem) to assess FXIIa.

FXIIa capture ELISA. FXIIa ELISA using B7 nanobodies was performed as previously described (20) with minor modifications. FXII was activated as described above, and kallikrein activity was inhibited by aprotinin. Activated FXII was added to citrated FXII-deficient plasma. Samples were taken over time and added to a stop mixture (0.5% w/v milk HBS [mHBS], 200 μM PPACK). The B7-coated plate was blocked with 2% mHBS, and detection antibodies were dissolved in 0.5% mHBS with 12.5 μM PPACK. ELISA wells coated with an unrelated nanobody were incubated identically and served as controls.

Biacore analysis. SPR analysis of C1INH-binding affinity to FXIIa was performed with Biacore T-200 Biosensor (GE Healthcare). N-terminal 6xHis-tagged FXIIa or FXIIa_Thr309Lys was captured on an NTA sensor chip, precharged with $NiCl_2$. C1INH (Berinert) association was measured for 120 seconds and dissociation for 60 sec-

onds before regeneration of the surface. C1INH was added in serial dilutions from 0.625 to 10 μM for detailed kinetics, with each concentration measured in duplicate. As N-terminal–tagged recombinant proteins were used, any small amounts of β fragment in the preparations would not bind to the chip surface and contaminate binding results. All assays were conducted at 37°C, and data were analyzed using the software provided by the manufacturer. Sensorgrams were double referenced by subtraction of signal from a reference flow cell and blank injections. Referenced sensorgrams were fitted to a heterogeneous ligand kinetic model with local R_{max} and association rate constants derived by least-squares fitting using Biacore T-200 evaluation software (GE Healthcare).

Real-time thrombin formation (endogenous thrombin potential) analysis. Thrombin generation in real time was analyzed by the calibrated automated thrombography (CAT) method of Hemker, using a Fluoroskan Ascent Fluorometer (Thermo Scientific) equipped with a dispenser (Thrombinoscope BV), with minor modifications (23). All experiments were run in triplicate in pooled normal platelet–poor human plasma or HAEIII patient plasma, both supplemented with 4 μM phospholipids. Plasma was activated with kaolin (1 μg/ml, Sigma-Aldrich) or ellagic acid (100 ng/ml, Actin FS, Siemens). Thrombin generation was calculated using the Thrombinoscope software package (version 3.0.0.29).

Expression of Thr309Lys-, Thr309Arg-, and Thr309Lys/Thr310Lys-mutated and WT FXII. FXII_Thr309Lys, FXII_Thr309Arg, and FXII_Thr309Lys/Thr310Lys site–directed mutagenesis (QuikChange Multi Site-Directed Mutagenesis Kit, Stratagene) was performed on human FXII cDNA (MIM ID: 610619) in a pcDNA3 vector with the following primers: 5′-CCGAAGCCTCAGCCCAAGACCCGGACCCCGCCTCAG-3′, 5′-CCGAAGCCTCAGCCCA**G**GACCCGGACCCCGCCTCAG-3′, and 5′-CCGAAGCCTCAGCCCA**A**GA**AG**CGGACCCCGCCTCAG-3′, resulting in the exchange of C at position 1032 to G (marked in bold; encoding for FXII_Thr309Arg) or A (marked in bold; encoding for FXII_Thr309Lys). C at position 1032 was mutated to A and CC at position 1035–1036 to AG (marked in bold) for FXII_Thr309Lys/Thr310Lys-coding cDNA. Transient transfection of FXII and the mutants into HEK293T cells (ATCC: CRL-3216) was done using Lipofectamine 2000 (Invitrogen) according to the manufacturer's instructions. The supernatant was collected 48 hours after transfection and concentrated with Amicon Ultra centrifugal filters (30 K, Millipore). In some experiments, FXII and the mutants were recombinantly expressed in HEK293T cells via a modified pcDNA6A V5 His vector (Invitrogen) and isolated via Strep-tag in combination with streptactin, according to the manufacturer's instructions (Streptactin Sepharose, IBA). Normal and mutated FXII variants containing an N-terminal 6xHis tag were similarly expressed in HEK293T cells but purified using Profility IMAC resins (Bio-Rad).

Vascular permeability assay. Vascular permeability assay was performed as described previously (24) with minor modifications; where indicated, *F12*$^{-/-}$ mice were preadministered recombinant FXII, FXII_Thr309Lys, or FXII_Thr309Arg (5 mg/kg bw), and some HAEIII transgene mice without doxycycline were pretreated with inhibitory FXIIa antibody 3F7 (7 mg/kg bw, ref. 23) or DX-88 (430 μg/kg bw). Densitometric scans of FXII signals in Western blots of blood samples collected over a week after infusion determined the half-life of recombinant human FXII transfused in *F12*$^{-/-}$ mice on a C57BL/6 background at 22 ± 8 hours.

Skin vascular leakage assay. Skin vascular permeability assay was performed as described previously (24) with minor modifications. Briefly, anesthetized mice were intravenously injected with 10 μl/g bw 0.25% Evans blue solution; 5 minutes later, 50 μl saline (negative control), BK (positive control, 100 μM, Sigma-Aldrich), or DXS (80 mg/ml, Sigma-Aldrich) was intradermally injected in the dorsal skin of mice using a 23-gauge syringe. After 30 minutes, the animals were sacrificed and the skin was removed and photographed. Skin samples were excised, and the Evans blue dye was extracted by incubation in N,N-dimethylformamide overnight at 55°C. After centrifugation at 10,000 *g* for 2 minutes, the supernatant was collected and the concentration of the extracted dye was determined by absorbance spectroscopy, λ at 620 nm.

$FeCl_3$-induced arterial thrombosis model. $FeCl_3$-induced arterial thrombosis model was performed as described previously (26) with minor modifications. The flow probe (Transonic Systems Inc.) was inserted around the carotid artery. A filter paper (1–2 mm) was saturated with 5% $FeCl_3$ and applied topically for 3 minutes. Challenged arteries were monitored for 40 minutes or until complete occlusion occurred (blood flow stopped for >10 minutes).

Transgene vector construct. FXII_Thr309Lys was cloned into a pTRE-Tight vector (Clontech Laboratories Inc./Takara Bio) to obtain pTRE-Tight_FXII_Thr309Lys.

Inducible FXII_Thr309Lys expression in cells. FXII_Thr309Lys was expressed using the reverse tetracycline-induced expressing system (Tet-On System). The transactivator plasmid expressed the reverse tTA under control of a CMV promoter, and the responder plasmid expressed TRE-controlled pTRE-Tight_FXII_Thr309Lys. In the presence of doxycycline (an analog to tetracycline), the transactivator binds to the responder plasmid TRE, allowing for expression of FXII_Thr309Lys. The transactivator plasmid and FXII_Thr309Lys vector were transfected into HEK293T cells using Lipofectamine 2000 in the presence of different concentrations of doxycycline (0.1–6.4 μg/ml). The supernatant was collected 48 hours after transfection, concentrated with Amicon Ultra centrifugal filters (30 K), and analyzed by Western blotting.

Generation of responder mouse strain (hFXII_Thr309Lys transgene) and doxycycline treatment. HAEIII transgene mice were generated using a transgenic mouse system with liver-specific inducible expression using the tetracycline-regulated expression system (Tet-Off System, Supplemental Figure 2A). This binary transgenic system involves 2 transgenic mouse lines. The first component is a mouse line that expresses the tTA under control of the LAP promotor (25) on a C57BL/6 background. Mice were purchased from Jackson Laboratories (Tg[Cebpb-tTA]5Bjd [tTA^{LAP}, LAP-tTA]). The second component is the responder mouse line that expresses mutant FXII (Thr309Lys) under the control of a TRE-driven minimal CMV promoter. The responder mouse line was generated via DNA microinjection of fertilized oocytes with the pTRE-Tight_FXII_Thr309Lys plasmid after linearization with *Bsp*HI (5′) and *Bsp*LU11I (3′), and mice were bred with tTA^{LAP} mice. Resulting double-transgenic animals were bred with *F12*$^{-/-}$ mice, leading to HAEIII mice. Genotyping of all mice was performed by PCR using the forward primer 5′-CGTATGTCGAGGTAGGCGTG-3′ and the reverse primer 5′-CACAAATGTACCCACAAGGGCCGGC-3′. The breeding scheme to obtain HAEIII mice is shown in Supplemental Figure 2B. The HAEIII mice possess an inducible mutated human FXII expression on the background of heterozygote endogenous FXII level. The standard rodent chow (Ssniff) was supplemented with doxy-

cycline (final concentration 100 mg/kg). Doxycycline was removed from mice 10 days before experiments were performed. Western blotting and aPTT analyses determined that combined plasma levels of mutant FXII and endogenous protein were similar to FXII plasma levels in WT animals. In plasma of doxycycline-fed animals, there was no FXII_Thr309Lys detectable by Western blotting (Figure 7B).

Statistics. All data are presented as mean ± SEM. Statistical analyses were performed with GraphPad Prism 5.0 software using unpaired 2-tailed Student's *t* test, and $P < 0.05$ was considered statistically significant.

Study approval. Animal care and experiments were approved by the Ethics Committee of Stockholm's Norra Djurförsöksetiska board. Mice were used between 6 and 12 weeks of age, and all strains were backcrossed to a C57BL/6 background for more than 10 generations. All plasma samples were obtained with written, informed consent under the approval of the research ethics committee of the city of Hamburg. Written, informed consent was provided for the clinical photograph.

Acknowledgments

We are grateful to Anna Sala-Cunill and Sven Cichon for donating plasma of HAEIII patients, Sandra Christiansen and Bruce Zuraw for providing the clinical photograph, and Hermann Bujard for providing tTA^{LAP} mice. We thank Sabine Wilhelm and Daniela Urlaub and Veronika Rayzman, Matt Hardy, and Min-Yin Yap for their excellent technical assistance. We are grateful to Lynn Butler for language editing. This work was supported in part by a Veni Fellowship (no. 016-126-159) provided by the Netherlands Organization for Scientific Research (NWO) to C. Maas. Financial support was also provided by the Ministerium für Innovation, Wissenschaft, und Forschung des Landes Nordrhein-Westfalen, by the Bundesministerium für Bildung und Forschung (to A. Sickman), Hjärt Lungfonden (20140741), Stockholms läns landsting (ALF, 20140464), Vetenskapsrådet (K2013-65X-21462-04-5), the German Research Society (SFB877, TP A11 and SFB841, TP B8), and a European Research Council grant (ERC-StG-2012-311575_F-12 to T. Renné).

Address correspondence to: Thomas Renné, Clinical Chemistry, Department of Molecular Medicine and Surgery, Karolinska Institutet, Karolinska University Hospital Solna (L1:00), SE-171 76 Stockholm, Sweden or Institute of Clinical Chemistry and Laboratory Medicine (O26), University Medical Center Hamburg-Eppendorf, Martinistrasse 51, D-20246, Hamburg, Germany. Phone: 0046.70.7730109; E-mail: thomas@renne.net.

1. Zuraw BL. Clinical practice. Hereditary angioedema. *N Engl J Med*. 2008;359(10):1027–1036.
2. Joseph K, Tuscano TB, Kaplan AP. Studies of the mechanisms of bradykinin generation in hereditary angioedema plasma. *Ann Allergy Asthma Immunol*. 2008;101(3):279–286.
3. Cugno M, Nussberger J, Cicardi M, Agostoni A. Bradykinin and the pathophysiology of angioedema. *Int Immunopharmacol*. 2003;3(3):311–317.
4. Schapira M, et al. Prekallikrein activation and high-molecular-weight kininogen consumption in hereditary angioedema. *N Engl J Med*. 1983;308(18):1050–1053.
5. Renne T, Schmaier AH, Nickel KF, Blomback M, Maas C. In vivo roles of factor XII. *Blood*. 2012;120(22):4296–4303.
6. Leeb-Lundberg LM, Marceau F, Muller-Esterl W, Pettibone DJ, Zuraw BL. International union of pharmacology. XLV. Classification of the kinin receptor family: from molecular mechanisms to pathophysiological consequences. *Pharmacol Rev*. 2005;57(1):27–77.
7. Bjorkqvist J, Sala-Cunill A, Renne T. Hereditary angioedema: a bradykinin-mediated swelling disorder. *Thromb Haemost*. 2013;109(3):368–374.
8. Han ED, MacFarlane RC, Mulligan AN, Scafidi J, Davis AE 3rd. Increased vascular permeability in C1 inhibitor-deficient mice mediated by the bradykinin type 2 receptor. *J Clin Invest*. 2002;109(8):1057–1063.
9. Zuraw BL, et al. Nanofiltered C1 inhibitor concentrate for treatment of hereditary angioedema. *N Engl J Med*. 2010;363(6):513–522.
10. Cicardi M, et al. Icatibant, a new bradykinin-receptor antagonist, in hereditary angioedema. *N Engl J Med*. 2010;363(6):532–541.
11. Cicardi M, et al. Ecallantide for the treatment of acute attacks in hereditary angioedema. *N Engl J Med*. 2010;363(6):523–531.
12. Bork K, Barnstedt SE, Koch P, Traupe H. Hereditary angioedema with normal C1-inhibitor activity in women. *Lancet*. 2000;356(9225):213–217.
13. Cichon S, et al. Increased activity of coagulation factor XII (Hageman factor) causes hereditary angioedema type III. *Am J Hum Genet*. 2006;79(6):1098–1104.
14. Dewald G, Bork K. Missense mutations in the coagulation factor XII (Hageman factor) gene in hereditary angioedema with normal C1 inhibitor. *Biochem Biophys Res Commun*. 2006;343(4):1286–1289.
15. Zuraw BL, et al. Hereditary angioedema with normal C1 inhibitor function: consensus of an international expert panel. *Allergy Asthma Proc*. 2012;33(suppl 1): S145–S156.
16. Citarella F, Ravon DM, Pascucci B, Felici A, Fantoni A, Hack CE. Structure/function analysis of human factor XII using recombinant deletion mutants. Evidence for an additional region involved in the binding to negatively charged surfaces. *Eur J Biochem*. 1996;238(1):240–249.
17. McMullen BA, Fujikawa K. Amino acid sequence of the heavy chain of human alpha-factor XIIa (activated Hageman factor). *J Biol Chem*. 1985;260(9):5328–5341.
18. Björkqvist J, Lecher B, Maas C, Renné T. Zinc-dependent contact system activation induces vascular leakage and hypotension in rodents. *Biol Chem*. 2013;394(9):1195–1204.
19. Joseph K, Tholanikunnel BG, Bygum A, Ghebrehiwet B, Kaplan AP. Factor XII-independent activation of the bradykinin-forming cascade: Implications for the pathogenesis of hereditary angioedema types I and II. *J Allergy Clin Immunol*. 2013;132(2):470–475.
20. de Maat S, van Dooremalen S, de Groot PG, Maas C. A nanobody-based method for tracking factor XII activation in plasma. *Thromb Haemost*. 2013;110(3):458–468.
21. Schousboe I. Binding of activated Factor XII to endothelial cells affects its inactivation by the C1-esterase inhibitor. *Eur J Biochem*. 2003;270(1):111–118.
22. Siebeck M, et al. Inhibition of plasma kallikrein with aprotinin in porcine endotoxin shock. *J Trauma*. 1993;34(2):193–198.
23. Larsson M, et al. A factor XIIa inhibitory antibody provides thromboprotection in extracorporeal circulation without increasing bleeding risk. *Sci Transl Med*. 2014;6(222):222ra17.
24. Oschatz C, et al. Mast cells increase vascular permeability by heparin-initiated bradykinin formation in vivo. *Immunity*. 2011;34(2):258–268.
25. Kistner A, et al. Doxycycline-mediated quantitative and tissue-specific control of gene expression in transgenic mice. *Proc Natl Acad Sci U S A*. 1996;93(20):10933–10938.
26. Renne T, et al. Defective thrombus formation in mice lacking coagulation factor XII. *J Exp Med*. 2005;202(2):271–281.
27. Miles AA, Miles EM. Vascular reactions to histamine, histamine-liberator and leukotaxine in the skin of guinea-pigs. *J Physiol*. 1952;118(2):228–257.
28. Bork K, Kleist R, Hardt J, Witzke G. Kallikrein-kinin system and fibrinolysis in hereditary angioedema due to factor XII gene mutation Thr309Lys. *Blood Coagul Fibrinolysis*. 2009;20(5):325–332.
29. Sala-Cunill A, et al. Plasma contact system activation drives anaphylaxis in severe mast cell-mediated allergic reactions. *J Allergy Clin Immunol*. 2015;135(4):1031–1043.
30. Donaldson VH, Evans RR. A Biochemical Abnormality in Herediatry Angioneurotic Edema: Absence of Serum Inhibitor of C' 1-Esterase. *Am J Med*. 1963;35:37–44.
31. Longhurst H, Cicardi M. Hereditary angio-oedema. *Lancet*. 2012;379(9814):474–481.
32. Marcos C, Lopez Lera A, Varela S, Linares T, Alvarez-Eire MG, Lopez-Trascasa M. Clinical,

biochemical, and genetic characterization of type III hereditary angioedema in 13 Northwest Spanish families. *Ann Allergy Asthma Immunol*. 2012;109(3):195–200.
33. Martin L, Raison-Peyron N, Nothen MM, Cichon S, Drouet C. Hereditary angioedema with normal C1 inhibitor gene in a family with affected women and men is associated with the p.Thr328Lys mutation in the F12 gene. *J Allergy Clin Immunol*. 2007;120(4):975–977.
34. Moreno AS, Arcuri H, Palma M, Arruda LKP. Structural and molecular changes caused by mutations Thr328Lys and Thr328Arg in FXII associated with hereditary angioedema with normal C1 inhibitor. *J Allergy Clin Immunol*. 2014;133(2):39.
35. Kaplan AP, Gruber B, Harpel PC. Assessment of Hageman factor activation in human plasma: quantification of activated Hageman factor-C1 inactivator complexes by an enzyme-linked differential antibody immunosorbent assay. *Blood*. 1985;66(3):636–641.
36. Bork K, Wulff K, Hardt J, Witzke G, Staubach P. Hereditary angioedema caused by missense mutations in the factor XII gene: clinical features, trigger factors, and therapy. *J Allergy Clin Immunol*. 2009;124(1):129–134.
37. Pathak M, et al. Coagulation factor XII protease domain crystal structure. *J Thromb Haemost*. 2015;13(4):580–591.
38. Cugno M, Cicardi M, Coppola R, Agostoni A. Activation of factor XII and cleavage of high molecular weight kininogen during acute attacks in hereditary and acquired C1-inhibitor deficiencies. *Immunopharmacol*. 1996;33(1–3):361–364.
39. Konings J, Cugno M, Suffritti C, Ten Cate H, Cicardi M, Govers-Riemslag JW. Ongoing contact activation in patients with hereditary angioedema. *PLoS One*. 2013;8(8):e74043.
40. Suffritti C, Zanichelli A, Maggioni L, Bonanni E, Cugno M, Cicardi M. High-molecular-weight kininogen cleavage correlates with disease states in the bradykinin-mediated angioedema due to hereditary C1-inhibitor deficiency. *Clin Exp Allergy*. 2014;44(12):1503–1514.
41. Stavrou EX, et al. Reduced thrombosis in Klkb1$^{-/-}$ mice is mediated by increased Mas receptor, prostacyclin, Sirt1, and KLF4 and decreased tissue factor. *Blood*. 2015;125(4):710–719.
42. Merkulov S, et al. Deletion of murine kininogen gene 1 (mKng1) causes loss of plasma kininogen and delays thrombosis. *Blood*. 2008;111(3):1274–1281.
43. Iwaki T, Castellino FJ. Plasma levels of bradykinin are suppressed in factor XII-deficient mice. *Thromb Haemost*. 2006;95(6):1003–1010.
44. Coffman LG, et al. Cleavage of high-molecular-weight kininogen by elastase and tryptase is inhibited by ferritin. *Am J Physiol Lung Cell Mol Physiol*. 2008;294(3):L505–L515.
45. Joseph K, Tholanikunnel BG, Kaplan AP. Factor XII-independent cleavage of high-molecular-weight kininogen by prekallikrein and inhibition by C1 inhibitor. *J Allergy Clin Immunol*. 2009;124(1):143–149.
46. Sartor RB, et al. Selective kallikrein-kinin system activation in inbred rats differentially susceptible to granulomatous enterocolitis. *Gastroenterology*. 1996;110(5):1467–1481.
47. Uknis AB, DeLa Cadena RA, Janardham R, Sartor RB, Whalley ET, Colman RW. Bradykinin receptor antagonists type 2 attenuate the inflammatory changes in peptidoglycan-induced acute arthritis in the Lewis rat. *Inflamm Res*. 2001;50(3):149–155.
48. Isordia-Salas I, et al. The mutation Ser511Asn leads to N-glycosylation and increases the cleavage of high molecular weight kininogen in rats genetically susceptible to inflammation. *Blood*. 2003;102(8):2835–2842.
49. Bork K, Wulff K, Meinke P, Wagner N, Hardt J, Witzke G. A novel mutation in the coagulation factor 12 gene in subjects with hereditary angioedema and normal C1-inhibitor. *Clin Immunol*. 2011;141(1):31–35.
50. Bork K, Wulff K, Hardt J, Witzke G. A deletion in the factor 12 gene analysed in two Turkish families with hereditary angioedema with normal C1 inhibitor (HAE type III): a Turkish F12 mutant. *Allergy*. 2013;68:15.
51. Kiss N, et al. Novel duplication in the F12 gene in a patient with recurrent angioedema. *Clin Immunol*. 2013;149(1):142–145.
52. Schloesser M, et al. Mutations in the human factor XII gene. *Blood*. 1997;90(10):3967–3977.
53. Hovinga JK, Schaller J, Stricker H, Wuillemin WA, Furlan M, Lammle B. Coagulation factor XII Locarno: the functional defect is caused by the amino acid substitution Arg 353-->Pro leading to loss of a kallikrein cleavage site. *Blood*. 1994;84(4):1173–1181.
54. Maas C, Oschatz C, Renne T. The plasma contact system 2.0. *Semin Thromb Hemost*. 2011;37(4):375–381.
55. Bjorkqvist J, Jamsa A, Renne T. Plasma kallikrein: the bradykinin-producing enzyme. *Thromb Haemost*. 2013;110(3):399–407.
56. Hojima Y, Cochrane CG, Wiggins RC, Austen KF, Stevens RL. In vitro activation of the contact (Hageman factor) system of plasma by heparin and chondroitin sulfate E. *Blood*. 1984;63(6):1453–1459.
57. Brunnee T, Reddigari SR, Shibayama Y, Kaplan AP, Silverberg M. Mast cell derived heparin activates the contact system: a link to kinin generation in allergic reactions. *Clin Exp Allergy*. 1997;27(6):653–663.
58. Seidel H, et al. Bleeding diathesis in patients with mast cell activation disease. *Thromb Haemost*. 2011;106(5):987–989.
59. Nzeako UC, Frigas E, Tremaine WJ. Hereditary angioedema: a broad review for clinicians. *Arch Intern Med*. 2001;161(20):2417–2429.
60. Maas C, et al. Misfolded proteins activate factor XII in humans, leading to kallikrein formation without initiating coagulation. *J Clin Invest*. 2008;118(9):3208–3218.
61. Kishimoto TK, et al. Contaminated heparin associated with adverse clinical events and activation of the contact system. *N Engl J Med*. 2008;358(23):2457–2467.
62. Siebeck M, et al. Dextran sulfate activates contact system and mediates arterial hypotension via B2 kinin receptors. *J Appl Physiol*. 1994;77(6):2675–2680.
63. Muller F, et al. Platelet polyphosphates are proinflammatory and procoagulant mediators in vivo. *Cell*. 2009;139(6):1143–1156.
64. Schmaier AH. The elusive physiologic role of Factor XII. *J Clin Invest*. 2008;118(9):3006–3009.
65. Matafonov A, et al. Factor XII inhibition reduces thrombus formation in a primate thrombosis model. *Blood*. 2014;123(11):1739–1746.
66. Mayforth RD, Quintans J. Designer and catalytic antibodies. *N Engl J Med*. 1990;323(3):173–178.
67. Chyung Y, et al. A phase 1 study investigating DX-2930 in healthy subjects. *Ann Allergy Asthma Immunol*. 2014;113(4):460–466.
68. Bhattacharjee G, et al. Inhibition of vascular permeability by antisense-mediated inhibition of plasma kallikrein and coagulation factor 12. *Nucleic Acid Ther*. 2013;23(3):175–187.
69. Revenko AS, et al. Selective depletion of plasma prekallikrein or coagulation factor XII inhibits thrombosis in mice without increased risk of bleeding. *Blood*. 2011;118(19):5302–5311.
70. Lewandrowski U, Zahedi RP, Moebius J, Walter U, Sickmann A. Enhanced N-glycosylation site analysis of sialoglycopeptides by strong cation exchange prefractionation applied to platelet plasma membranes. *Mol Cell Proteomics*. 2007;6(11):1933–1941.
71. Renne T, Dedio J, David G, Muller-Esterl W. High molecular weight kininogen utilizes heparan sulfate proteoglycans for accumulation on endothelial cells. *J Biol Chem*. 2000;275(43):33688–33696.
72. Renne T, Dedio J, Meijers JC, Chung D, Muller-Esterl W. Mapping of the discontinuous H-kininogen binding site of plasma prekallikrein. Evidence for a critical role of apple domain-2. *J Biol Chem*. 1999;274(36):25777–25784.